

We appreciate having received detailed comments from the reviewers. We have revised the manuscript accordingly. Below, you will find our response and the summary of our approach, highlighted in *red*, with modifications to the manuscript highlighted *in bold*:

Referee #1:

This paper discusses observed light extinction of nominally PM₂ particles measured over the Colorado Front Range during the FRAPPE aircraft study. The authors assert that this paper provides an updated assessment on the Denver Brown Cloud. This is a worthwhile topic and the paper is suitable for publication in ACP. However, there are number logical inconsistencies, important missing information, and other issues that must be addressed, including:

-particle size range and RH of the extinction measurement is not well characterized making the data of questionable value (ie, how to compare to other studies and how to apply to ambient conditions).

The reviewer has raised a good point. We have estimated the RH in the CAPS-PM_{ex} unit, using the measured ambient temperature and RH assuming aerosols had equilibrated to the temperature within the instrument. Our results indicate that on average the RH in the CAPS was $20 \pm 7\%$ with a range of 15-30% while ambient RH was on average $44 \pm 17\%$.

We have addressed this issue in section 2.2, paragraph 4 by adding the following sentences: “Based on the ambient RH and temperature and the temperature within the CAPS-PM_{ex} extinction cell, and assuming that aerosols had equilibrated to the conditions within the measurement cell, the CAPS-PM_{ex} measurements for the flights discussed here represent extinction values at an average RH of $20 \pm 7\%$ (range of 15-30%).”

-mismatch between AMS and extinction measured particle size ranges.

In order to determine whether the discrepancy between the aerosol size ranges being sampled by the CAPS-PM_{ex} and AMS had a significant impact on our analysis or not, we have used the size distributions from the Passive Cavity Aerosol Spectrometer Probe (PCASP) instrument on board the C-130 to estimate the ambient scattering coefficients. By using a nominal refractive index of 1.5, estimated scattering (i.e., extinction, while assuming purely scattering aerosols) coefficients were calculated using the measured size distributions up to 800 nm (upper “true” size cut of the AMS) and 2000 nm (upper size cut of the inlet, and thus CAPS-PM_{ex}). The slopes of the scatter plots of the estimated scattering coefficients for PM_{0.8} vs. PM₂ under the influence of urban, O&G, agricultural, and urban+O&G slopes were 0.95 ± 0.01 , 1.0 ± 0.002 , and 1.0 ± 0.01 , 0.92 ± 0.01 , respectively, indicating that the majority of the signal contribution to extinction originated from aerosols in the size range of the mAMS. We also note that the slope values mentioned above were not highly sensitive to the choice of the refractive index. Changing the refractive index from 1.48 to 1.52 changed the slope values by at most 4%.

The following has been added to the text in section 2.2, paragraph 3 to address this issue: “Ambient aerosol size distributions were measured on-board the C-130 by a Passive Cavity Aerosol Spectrometer Probe (PCASP). Estimated extinction values using Mie calculations with a nominal refractive index of 1.5 and the measured PCASP size distributions indicated that particles smaller than 800 nm captured >92% of PM₂ extinction values, confirming that the majority of the extinction signal originated from aerosols in the size range of the mAMS. We note that the calculated extinction coefficients were not highly sensitive to the choice of refractive index; only a 4% decrease in the slope of scattering coefficients from PM_{0.8} vs. PM₂ was observed by increasing the refractive index from 1.48 to 1.52.”

-the justification for the use of extinction versus CO to compare extinction versus photochemical age for all combined sources.

We agree with the reviewer that it makes more sense to limit the data in Figure 2 to plume types where aerosol precursors are co-emitted with CO. Therefore, Figure 2 has now been updated to include data from urban emissions only, with the modified definition provided in Section 3.1 as "...plumes with enhancement of CO over the background (105 ppbv, as defined by the mode in the frequency distribution of CO in the Front Range boundary layer) while $\Delta C_2H_6/\Delta CO < 20$ pptv ppbv⁻¹). We also had to remove data from July flights due to lack of optimum quantitative quality of CO data during those flights, that was reflected on the data archive site after initial submission of the paper. With these changes, aging categories needed to be updated to $NO_x:NO_y > 0.5$ and < 0.5 to represent relatively fresh and aged plumes, respectively, in order to include enough data points in each category. Despite these changes, the conclusions remain the same that with the reduction in $NO_x:NO_y$ and increase in photochemical aging, the enhancement ratio of $\Delta\beta_{ext}/\Delta CO$ increased significantly (by ~54%).

Also, given the discussion in the Introduction that the motivation of this work was to take a new look at the Denver Brown cloud, it is rather odd that this is never done. It would be insightful to add a section on comparing/contrasting these results to earlier studies; has visibility improved, have sources that contribute to visibility reduction changed, etc.

Since summertime extinction data from previous field studies in the Colorado Front Range are not available, we have used transmissometer extinction data, provided by the Colorado Department of Public Health, to consider monthly average values of extinction measured in Downtown Denver for the months of July and August during 2001-2014.

We have included the following sentences in section 3.3, paragraph 4 describing the observations: "In response to the wintertime haze episodes observed in the region, the State of Colorado has implemented a visibility standard based on total optical extinction of 76 Mm^{-1} at 550 nm, averaged during a 4-hr period when ambient RH is less than 70% (Ely et al. 1993). Total optical extinction measurements are provided by the Colorado Department of Public Health and Environment's transmissometer, installed in Downtown Denver. We have assessed the average monthly total extinction coefficients for August of 2001-2014 to examine the recent trend in summertime extinction and visibility in the region. Averaged monthly values varied from 40 to 80 Mm^{-1} , and no significant trend was observed since 2001."

Specific comments:

Why is there no discussion of any anthropogenic gases that may contribute to the Denver Brown Cloud, either in past studies or this study? Are they not important (give numbers to support). Are they included in the reported extinction measurement, or subtracted out with the blank correction?

Based on wintertime optical extinction measurements in 1978, (Groblicki et al. 1981) estimated that gaseous scattering and NO_2 absorption each contributed to 7% of total extinction at 550 nm. As described in Section 2.2, CAPS- PM_{ex} provides only measurements of aerosol optical extinction since frequent filtered-air samples are collected during normal operation to subtract the background gaseous contributions to extinction. Following Groblicki's derivation of absorption coefficient at 550 nm using NO_2 mixing ratios and since NO_2 absorption cross section at 632 nm is about $10\times$ lower than at 550 nm (Schneider et al, 1987), estimated average NO_2 absorption at 632 nm in the Front Range was less than 0.1 Mm^{-1} . Therefore, although the reported measurements of extinction are for aerosol particles, contribution of anthropogenic gases to total extinction at 632 nm in the Front Range is negligible.

The following has been added to Section 2.2: "It is worth reiterating that anthropogenic gases such as nitrogen dioxide have minimal effect on the measured β_{ext} at 632nm since regular baseline

corrections based on sampled filtered air were applied to the data. Given the average mixing ratio of NO₂, the parameterization by Groblicki et al. (1981) for estimating NO₂ absorption at 550 nm, and the factor of 10 smaller value of NO₂ absorption cross section at 632 nm compared to 550 nm (Schneider et al, 1987), we estimated the average absorption of NO₂ to be ~0.1 Mm⁻¹, indicating a minor contribution of NO₂ to total extinction at 632 nm.”

Page 3 and throughout; specifically note that the altitudes give are above sea level (I assume), not surface?

In section 2.1, we have now noted that altitude is above sea level.

Page 4, line 18; the CAPs(ext) did not have a size selective inlet; apparently upper size limit is controlled by only inlet/sample line transmission efficiencies? Discuss in more detail, specifically how well is the size range of particles contributing to the measured extinction really known (give the uncertainty, my suspicion is that it is large of it is bases solely on calculated inlet and sample line transmissions). What are the implications of this uncertainty (the size distribution was measured so a quantitative estimate should be possible). How does one handle the mismatch in particle sizes sampled with the AMS and CAPs? This could have impacts on much of the reported data, depending on the shape of the size distribution. Add a discussion.

Since the data presented in the manuscript were limited to the boundary layer, variations in the transmission efficiency of the inlet were really minor. We have calculated transmission efficiency of the inlet given a range of ambient pressures (760-860 mbar) and ambient temperatures (15-30 °C) representative of the BL; the 50% size cut for these conditions was 2.05± 0.05 μm. As further discussed below, most of the signal contribution to aerosol extinction was from much smaller particles (<800 nm), so minor variations in the transmission of ~2 μm particles could not pose significant uncertainties in the measurements.

In order to determine whether the discrepancy between the aerosol size ranges being sampled by the CAPS-PM_{ex} and AMS had a significant impact on our analysis or not, we have used the size distributions from the Passive Cavity Aerosol Spectrometer Probe (PCASP) instrument on board the C-130 to estimate the ambient scattering coefficients. By using a nominal refractive index of 1.5, estimated scattering (i.e., extinction, while assuming purely scattering aerosols) coefficients were calculated using the measured size distributions up to 800 nm (upper “true” size cut of the AMS) and 2000 nm (upper size cut of the inlet, and thus CAPS-PM_{ex}). The slopes of the scatter plots of the estimated scattering coefficients for PM_{0.8} vs. PM₂ under the influence of urban, O&G, agricultural, and urban+O&G slopes were 0.95 ± 0.01, 1.0 ± 0.002, and 1.0 ± 0.01, 0.92± 0.01, respectively, indicating that the majority of the signal contribution to extinction originated from aerosols in the size range of the mAMS. We also note that the slope values mentioned above were not highly sensitive to the choice of the refractive index. Changing the refractive index from 1.48 to 1.52 changed the slope values by at most 4%.

The following has been added to the text in section 2.2, paragraph 3 to address this issue: “Ambient aerosol size distributions were measured on-board the C-130 by a Passive Cavity Aerosol Spectrometer Probe (PCASP). Estimated extinction values using Mie calculations with a nominal refractive index of 1.5 and the measured PCASP size distributions indicated that particles smaller than 800 nm captured >92% of PM₂ extinction values, confirming that the majority of the extinction signal originated from aerosols in the size range of the mAMS. We note that the calculated extinction coefficients were not highly sensitive to the choice of refractive index; only a 4% decrease in the slope of scattering coefficients from PM_{0.8} vs. PM₂ was observed by increasing the refractive index from 1.48 to 1.52.”

No discussion on RH (or T) of sample in the CAPS? RH variability could have a large effect on extinction. In the paper it is referred to as dry extinction, but RH is never given? It appears that the authors are just assuming the particles are dry since the ambient RH was low and the particles heated in

the inlet/sample line. Much more detail, along with possible differences in LWC of sampled and ambient aerosol, should be considered. Note, at the least one could estimate the RH in the CAPS assuming the aerosol has reached cabin T, if one knows the ambient RH and T. Claiming a dry extinction measurement really requires reporting actual RH in the CAPs.

The reviewer has raised a good point. We have estimated the RH in the CAPS-PM_{ex} unit, using the measured ambient temperature and RH assuming aerosols had equilibrated to the temperature within the instrument. Our results indicate that on average the RH in the CAPS was 20 ± 7% with range of 15-30% while ambient RH was on average 44±17%.

We have addressed the issue on RH in section 2.2 paragraph 4 by adding the following sentences: “Based on the ambient RH and temperature and the temperature within the CAPS-PM_{ex} extinction cell, and assuming that aerosols had equilibrated to the conditions within the measurement cell, the CAPS-PM_{ex} data discussed here represent extinction values at an average RH of 20 ± 7 % (range of 15-30%)”.

Page 4 line 22, typo, intends or just tends?

The sentence has been rephrased.

Re. Fig 2 and the general idea of looking at extinction vs CO: The logic behind the graph and more details may be needed. First, is this data just for well defined plumes or include all data, except biomass burning (ie, it includes urban and agri, urban+O&G, and O&G)? Second, this plot is predicted on a correlation between extinction and CO; that is that the components driving extinction and CO are co-emitted in all sources included in this plot. This appears to be the case, but it is curious why this is so if it includes all these various sources. That is, if this plot is for all sources combined, why do they all have similar Ext/CO ratios (ie, only a function of age)? Maybe this plot is mainly driven by urban emissions. This would also mean that most of the aging is just due to OA aging. Fig 3 would support this, in a general sense. Why not use a PMF analysis and look at evolution of specific AMS OA factors? Why lump all the data together in this plot since it is more valid for a plume from a specific source; wouldn't graphs like this for each specific source make more sense, or maybe just focus on the urban data? Also, one would expect that some components that contribute to extinction, such as sulfate and nitrate would not be correlated with CO and so not appropriate to include sources with high emissions of these components in this analysis. Maybe this accounts for much of the scatter? One might also give the overall r² between extinction and CO (ie not segregated by age) in Fig 2, and finally, why the different intercepts in Fig 2?

We agree with the reviewer that it makes more sense to limit the data in Figure 2 to plume types where aerosol precursors are co-emitted with CO. Therefore, Figure 2 has now been updated to include data from urban emissions only, with the modified definition provided in Section 3.1 as “...plumes with enhancement of CO over the background (105 ppbv, as defined by the mode in the frequency distribution of CO in the Front Range boundary layer) while $\Delta C_2H_6/\Delta CO < 20$ pptv ppbv⁻¹). We also had to remove data from July flights due to lack of optimum quantitative quality of CO data during those flights, that was reflected on the data archive site after initial submission of the paper. With these changes, aging categories needed to be updated to $NO_x:NO_y > 0.5$ and < 0.5 to represent relatively fresh and aged plumes, respectively, in order to include enough data points in each category.

Carrying out PMF analysis is outside the scope of this paper.

Indeed the correlation coefficients improved from $r \sim 0.6-0.7$ to $r \sim 0.85-0.9$, when excluding the non-urban plumes from this plot, confirming that some species that contributed to β_{ext} were not co-emitted with CO.

The different intercepts observed when considering all plume types would have suggested different background levels of β_{ext} due to inclusion of all aerosol source types in the plot. With the current

modification of including data from only the urban plumes, the fresh and aged fitted lines cross similar β_{ext} values (6.0-6.7 Mm^{-1}) at the background CO level of 105 ppbv.

Fig 3, any estimates on potential bias in the composition data due to sampling only submicron non-refractory aerosol with the AMS? In some sources this could lead to substantial bias, eg, the AMS would not measure more refractory nitrate salts that could be present in some of the sources (eg, $NaNO_3$, $Ca(NO_3)_2$, : : :).

On average, less than $0.5 \mu g/m^3$ of Ca^{2+} plus Mg^{2+} (Na^+ concentrations were not reported) was present in the PM_{10} aerosols as measured by a PILS aboard the C130; therefore, contribution of refractory salts is not expected to be significant.

Why is there so much OA associated with agri emissions?

The organics that were associated with aerosols observed in agricultural plumes were not originating from agriculture emissions since no significant enhancement in OA was observed while crossing such plumes. Therefore, the organics merely represent the composition of the background aerosol onto which agricultural emissions were superimposed.

Page 6 last line, the assumption is being made that nitrate formation is controlled by NH_3 concentrations through partitioning of nitric acid. What is the justification for this?

The process is actually likely to be much more complicated as it depends on the pH of the aerosol, which in turn depends on the amount of mineral dust and sulfate also present; it doesn't just depend on NH_3 concentration. Also, given that NH_3 was measured, one could be more specific and quantify the differences in NH_3 levels in the various source regions.

It is true that formation of ammonium nitrate depends on aerosol pH and other components of aerosol. As mentioned above, dust components of aerosol based on PILS data were minor. Additionally, AMS composition indicates that chloride and sulfate levels were very uniform in different air masses. The most variable parameter that could have an impact on aerosol composition was NH_3 levels, with average values of 1.41 ± 1.2 ppbv, 2.75 ± 1.88 ppbv, 8.21 ± 2.06 ppbv, and 5.47 ± 1.81 ppbv in urban, O&G, agriculture, and urban+O&G plumes, respectively. The following has been added in Section 3.2 to support our hypothesis: "Aerosol nitrate formation depends on ambient conditions (temperature and relative humidity), relative mixing ratios of nitric acid and ammonia, as well as aerosol composition and pH (Seinfeld and Pandis 2006, Weber et al. 2016). With uniform concentrations of sulfate aerosol and small contribution of chloride and dust components to the Front Range fine aerosol mass, variability in aerosol pH was not expected to be high. Furthermore, there was no specific trend in temperature or relative humidity in different plume types. On the other hand, mixing ratios of ammonia were observed to be variable in the different air masses, with average values of 1.41 ± 1.2 ppbv, 2.75 ± 1.88 ppbv, 8.21 ± 2.06 ppbv, and 5.47 ± 1.81 ppbv in urban, O&G, agriculture, and urban+O&G plumes, respectively."

Fig 6, how can there be so few particles (generally less than 40 or so particles per cm^3 of air, get mass concentrations are up to 15 to 20 $\mu g/m^3$? Seems very odd.

The reviewer might have misread the horizontal axis in Fig 6. The axis represents the number of aerosol particles in 300-2000 nm size range and not the total number of fine aerosols. The low number of aerosols in the larger size bins just indicates that the majority of ambient particles were at sizes smaller than 300 nm, which is typically the case. This figure is no longer included in the manuscript.

Fig 8, the correlations are not that good, total mass explains only 25 to 35% of the extinction variability (r^2), so are the regressions really meaningful (comparisons of slopes for each plot)?

We have updated this Figure to include data with masks designating the 4 plume types that have been examined in detail in the paper. This has greatly improved the correlations of b_{ext} and NR-PM₁ mass, with r values ~ 0.75 , as well as the trends of the weighted ODR fits. Please note that because BB also contributes to atmospheric CO, we decided the conclusions drawn from the scatter plot of β_{ext} vs. CO in the presence and absence of BB could not be as robust as desired and have therefore deleted panel b.

The following text in Section 3.4 has been updated accordingly: "MEE values were analyzed for days with and without the BB influence, using weighted linear ODR fit analysis, as explained previously. As seen in Figure 8, average MEE on Aug. 11-12 was $\sim 70\%$ greater compared to days without the influence of BB (3.65 ± 1.16 m²/g vs. 2.24 ± 0.71 m²/g). Additionally, during Aug. 11-12, background value of airborne β_{ext} was higher at 4.00 ± 0.71 Mm⁻¹ compared to 0.25 ± 0.11 Mm⁻¹ on days without the BB influence, suggesting the additional contribution to β_{ext} from the wildfires."

References

Ely, D. W., et al. (1993). The establishment of the Denver visibility standard. Air And Waste Management Association Annual Meeting, Air And Waste Management Association. **1**.

Groblicki, P. J., et al. (1981). "Visibility-Reducing Species in the Denver "Brown Cloud"- I. Relationships between Extinction and Chemical Composition." Atmos. Env. **15**(12): 2473-2484.

Seinfeld, J. H. and S. N. Pandis (2006). Atmospheric chemistry and physics: from air pollution to climate change. Hoboken, New Jersey, John Wiley and Sons, Inc.

Weber, R. J., et al. (2016). "High aerosol acidity despite declining atmospheric sulfate concentrations over the past 15 years." Nature Geoscience **9**(4): 282-+.

We appreciate having received detailed comments from the reviewers. We have revised the manuscript accordingly. Below, you will find our response and the summary of our approach, highlighted in *red*, with modifications to the manuscript highlighted *in bold*:

Referee #2:

Review of Aerosol Optical Extinction during the Front Range Air Pollution and Photochemistry Experiment (FRAPPÉ) 2014 Summertime Field Campaign, Colorado U.S.A.

Overall Comments This paper describes relationships between mass measurements from the mAMS and extinction measurements from a CAPS-PM_{ex} instrument in the Front Range of Colorado. The authors derive Mass Extinction Efficiencies for a number of different airmass types (urban, oil and gas, agricultural) based on gas-phase tracer measurements from the study. The paper presents some interesting, relevant results and is appropriate for publication in ACP after some significant revisions described below. The major problems with the submitted manuscript are

- 1.) The error estimates for the CAPS-PM_{ex} are not explained or justified for this study, only a reference is given. The error estimate of 10% seems much too small for small extinction measurements (<10 Mm⁻¹) given that the authors observed significant baseline shifts.

*The frequency distribution plot of the difference in the consecutive baseline values shows that 72% (88%) of the times, baseline shift was within 0.5 Mm⁻¹ (1 Mm⁻¹). Regardless, after reviewing our procedures for preparing the final version of the CAPS-PM_{ex} data, we realized that we had actually interpolated the baseline values throughout the mission! It was a complete oversight on our part that we didn't explain the procedure for baseline correction accurately in the submitted version. The correct approach is now updated in Section 2.2: **"Although for majority (72%) of the data, consecutive baseline values had shifted by less than 0.5 Mm⁻¹, baseline values were interpolated for a more accurate estimation of optical extinction."***

*The stated 1-s detection limit for CAPS-PM_{ex} was from one of the original papers by Massoli et al. (Massoli et al. 2012). Examining the standard deviations of the measured extinction coefficients during filtered ambient air sampling periods during the project actually indicated a lower 1-s detection limit of ~1.5 Mm⁻¹ (assuming 3-σ). The estimate of the detection limit and the corresponding time are now updated in Section 2.2: **"The estimated uncertainty in β_{ext} is 10%, while the 3-σ detection limit for 1-s data under particle free air for the conditions encountered during FRAPPE was ~1.5 Mm⁻¹ (Massoli et al. 2010, Petzold et al. 2013)"**.*

In general, accuracy of the CAPS-PM_{ex} measurements depends on the accuracy of the baseline and the geometry correction factor (i.e., to know the purge effects). Accuracy in this factor is mostly limited by the accuracy of the CPC during calibrations, which if calibrated carefully with an electrometer, is on the order of ±4%. Considering some uncertainty is also associated with the interpolated baseline values (see our response above regarding baseline correction), we believe an overall 10% uncertainty in the extinction coefficient is conservative, but reasonable.

- 2.) The authors see poor correlation between mass measured by the AMS and extinction. This poor correlation is stated to be due to changes in size distribution. However, in some of the plume types, especially urban, there does not appear to be a dramatic difference in the size-distribution of low and high MEE plumes. If the authors are going to conclude that size distribution is responsible for widely varying MEE, this needs to be backed up with some Mie modeling that shows the observed shifts in size

distribution can cause the observed shifts in MEE. It is also possible that varying size cutpoints between the mAMS and CAPS-PM_{ex} are significant and this needs to be discussed. Additional comments are given below.

In order to determine whether the discrepancy between the aerosol size ranges being sampled by the CAPS-PM_{ex} and AMS had a significant impact on our analysis or not, we have used the size distributions from the Passive Cavity Aerosol Spectrometer Probe (PCASP) instrument on board the C-130 to estimate the ambient scattering coefficients. By using a nominal refractive index of 1.5, estimated scattering (i.e., extinction, while assuming purely scattering aerosols) coefficients were calculated using the measured size distributions up to 800 nm (upper “true” size cut of the AMS) and 2000 nm (upper size cut of the inlet, and thus CAPS-PM_{ex}). The slopes of the scatter plots of the estimated scattering coefficients for PM_{0.8} vs. PM₂ under the influence of urban, O&G, agricultural, and urban+O&G slopes were 0.95 ± 0.01 , 1.0 ± 0.002 , and 1.0 ± 0.01 , 0.92 ± 0.01 , respectively, indicating that the majority of the signal contribution to extinction originated from aerosols in the size range of the mAMS. We also note that the slope values mentioned above were not highly sensitive to the choice of the refractive index. Changing the refractive index from 1.48 to 1.52 changed the slope values by at most 4%.

The following has been added to the text in section 2.2, paragraph 3 to address this issue: “Ambient aerosol size distributions were measured on-board the C-130 by a Passive Cavity Aerosol Spectrometer Probe (PCASP). Estimated extinction values using Mie calculations with a nominal refractive index of 1.5 and the measured PCASP size distributions indicated that particles smaller than 800 nm captured >92% of PM₂ extinction values, confirming that the majority of the extinction signal originated from aerosols in the size range of the mAMS. We note that the calculated extinction coefficients were not highly sensitive to the choice of refractive index; only a 4% decrease in the slope of scattering coefficients from PM_{0.8} vs. PM₂ was observed by increasing the refractive index from 1.48 to 1.52.”

Upon closer examination, it became apparent that correlations between β_{ext} and neither of the non-refractory AMS species were high in the urban plumes while as shown in Figure 2, β_{ext} and CO were strongly correlated ($r > 0.85$). We suspect that BC emissions in urban plumes, which are indeed not included in NR-PM₁, actually played a role in controlling β_{ext} , especially in fresh plumes. It is therefore not surprising that the overall correlation of β_{ext} vs. NR-PM₁ in Figure 5a was also not high. The related paragraph in Section 3.2 is now updated to reflect these observations: “The scatter plots of dry β_{ext} vs. OA under urban, O&G, and urban + O&G air masses presented correlation coefficients of $r = 0.46$, 0.72 , 0.46 , respectively. This observation suggests that O&G emissions are important for organic aerosol contribution to β_{ext} . On the other hand, in urban plumes, the correlation between β_{ext} and OA was lower than in O&G plumes while as demonstrated in Figure 2, β_{ext} and CO were strongly correlated under both fresh and aged air masses. These observations suggest that species other than OA, e.g., black carbon, that are co-emitted with CO are also important in driving β_{ext} in urban-influenced air masses.”

Comments on Introduction

1.) It is stated that, “it has been observed that the important contributors to light scattering in the Colorado Rocky Mountains are particulate matter from the urban emissions” Certainly there are dust and smoke events that cause visibility degradation too, in fact the authors show a smoke event. This statement is far too broad.

This sentence has been modified to express the influence of anthropogenic emissions on visibility: “For example, it has been observed that the important anthropogenic contributors to light scattering in the Colorado Rocky Mountains are particulate matter from the urban emissions (Levin et al. 2009)”.

2.) The authors discuss the wintertime phenomenon of the Denver Brown Cloud but do not discuss summertime visibility issues. Some background on typical extinction or at least PM_{2.5} mass in the summertime in Denver is needed.

The last comprehensive aerosol composition measurement study dates back to 1996 while Optical extinction data from the past field studies are not available. After contacting the Colorado Department of Public Health and Environment, we have obtained data on total optical extinction (550 nm) from the transmissiometer measurements in downtown Denver for August 2001-2014. The following section has been added to Introduction to highlight the most recent summertime observations of PM_{2.5} composition and extinction: “Previous measurements of summertime particle composition in the Colorado Front Range were conducted during the Northern Front Range Air Quality Study (NFRAQS) between July 17 to August 31, 1996 at several urban and rural sites. The major components of PM_{2.5} mass were identified to be carbonaceous and inorganic aerosols, with carbonaceous aerosols contributing to about 46% of PM_{2.5} mass. The 24-hour average measurements of PM_{2.5} organic carbon, nitrate, and sulfate particles were observed to be 4.2 µg/m³, 0.9-1.2 µg/m³, and 1.4-1.5 µg/m³, respectively (Watson et al. 1998). In response to the wintertime haze episodes observed in the region, the State of Colorado has implemented a visibility standard based on total optical extinction of 76 Mm⁻¹ at 550 nm, averaged during a 4-hr period when ambient RH is less than 70% (Ely et al. 1993). Total optical extinction measurements are provided by the Colorado Department of Public Health and Environment’s transmissiometer installed in Downtown Denver. The average total extinction values of August 2001-2014, ranging from 40-80 Mm⁻¹, reveal no significant trend in summertime extinction and visibility in the region since 2001.”

3.) The statement “twofold increase in natural resource extraction” is vague. Is this an increase in wells, in gas production, in oil production? This is relevant because each has a different implication for air quality.

The twofold increase refers to the number of wells in the regions. We have now added a few sentences in section 1 paragraph 3 of the introduction section, that specifically list the sources of fossil fuel production and various related operations. “With a twofold increase in natural resource extraction wells since 2005 to about 24,000 active oil and natural gas (O&G) production wells in 2012, northeastern Colorado has experienced extensive fossil fuel production within the past decade (Scamehorn 2002, Pétron et al. 2014). This includes increases in fossil fuel production from coal bed methane, tight sand and shale natural gas, shale oil, and the associated gases. The emissions from these processes have several environmental impacts such as greenhouse emissions of methane and emissions of non-methane hydrocarbons that impair air quality. Emissions from diesel trucks, drilling rigs, power generators, phase separators, dehydrators, storage tanks, compressors and pipes used in O&G operations also contribute to the regional burden of volatile organic compounds (VOCs), nitrogen oxides, and particulate matter (i.e., black carbon and primary organic carbon) (Gilman et al. 2013).”

4.) The authors state that emissions from oil and gas include “emissions from industrial equipment known to emit. . .particulate matter.” Are they referring to BC from diesel engines? There needs to be clarification here because there are not typically large primary emissions of particulate matter from oil and gas operations.

As with any off-road diesel equipment, PM emissions from such sources could include BC and POA. This is now clarified as “Emissions from diesel trucks, drilling rigs, power generators, phase separators, dehydrators, storage tanks, compressors and pipes used in O&G operations also contribute to the regional burden of volatile organic compounds (VOCs), nitrogen oxides, and particulate matter (i.e., black carbon and primary organic carbon) (Gilman et al. 2013).”

5.) I don't see a basis for the authors to conclude that photochemical production of ozone is significantly impacted by oil and gas operations. There's a big jump from OH reactivity in the winter to ozone production in the summer and no evidence to back up this logical leap. This also has little to do with the paper, I would suggest removing the last line of page 2 and the first line of page 3.

The sentence was removed accordingly.

Comments on Instrumentation and Methodology

1.) The description of the CAPSPM_{ex} operating principles is fairly poor. It makes it seem that the extinction is detected by monitoring the phase shift that occurs during 1 transit of the light from the first mirror to the second. This is far from accurate, the entire point of the instrument is to create a very long effective pathlength.

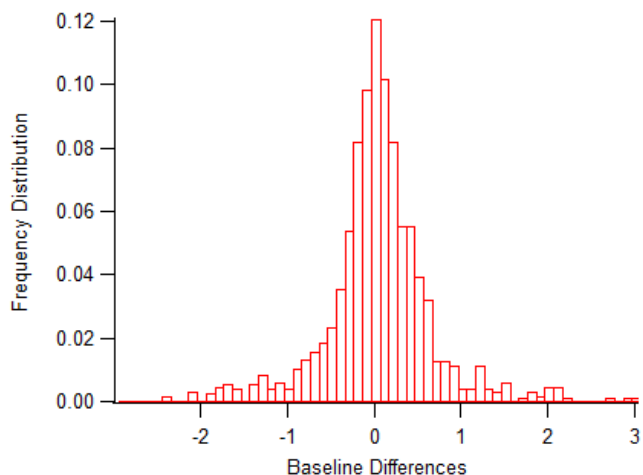
It was not our intention to suggest such a short path-length of light within the CAPS instrument. Additional information on the CAPS-PM_{ex} effective path length are now included in Section 2.2. of the manuscript. "Within the optical cell cavity, the highly reflective mirrors create an effective path length of approximately 2 km. Under the particle free sampling mode, the light emitting diode (LED) light output is directed to the first mirror, while a small fraction goes through the second mirror to the photodiode detector, producing a slightly distorted waveform of the square-wave modulated by the LED, whereas under the aerosol sampling mode, the detector detects a greater distorted waveform, characterized by a phase shift. The vacuum photodiode, which is located behind the second reflective mirror detects and measures that phase shift when the square wave becomes distorted due to interactions with sampled air under a relatively long effective path length."

2.) Line 4 page 4: An averaging time needs to be given for uncertainty and detection limit statements.

The stated 1-s detection limit for CAPS-PM_{ex} was from one of the original papers by Massoli et al. (Massoli et al. 2012). Examining the standard deviations of the measured extinction coefficients during filtered ambient air sampling periods during the project actually indicated a lower 1-s detection limit of ~1.5 Mm⁻¹ (assuming 3-σ). The estimate of the detection limit and the corresponding time are now updated in Section 2.2: "The estimated uncertainty in β_{ext} is 10%, while the 3-σ detection limit for 1-s data under particle free air for the conditions encountered during FRAPPE was ~1.5 Mm⁻¹ (Massoli et al. 2010, Petzold et al. 2013)".

3.) Why were baseline values only interpolated when the shift was more than 5 Mm⁻¹? I see no reason not to always interpolate them. It also needs to be explained why the baseline would shift that much. Given that most reported measurements are <20 Mm⁻¹, this would seem to be a big issue.

The following frequency distributions plot of the difference in the consecutive baseline values shows that 72% (88%) of the times, baseline shift was within 0.5 Mm⁻¹ (1 Mm⁻¹). Regardless, after reviewing our procedures for preparing the final version of the CAPS-PM_{ex} data, we realized that we had actually interpolated the baseline values throughout the mission! It was a complete oversight on our part that we didn't explain the procedure for baseline correction accurately in the submitted version.



The correct approach is now updated in Section 2.2: “Although for majority (72%) of the data, consecutive baseline values had shifted by less than 0.5 Mm^{-1} , baseline values were interpolated for a more accurate estimation of optical extinction.”

4.) Error analysis for the CAPS seems to need significantly more attention in general. 10% is clearly not a correct estimate of error in the extinction coefficient when the average extinction is something around 15 Mm^{-1} and you have a baseline shift of 5 Mm^{-1} . The authors need to do a careful assessment of error in the extinction measurement.

In general, accuracy of the CAPS- PM_{ex} measurements depends on the accuracy of the baseline and the geometry correction factor (i.e., to know the purge effects). Accuracy in this factor is mostly limited by the accuracy of the CPC during calibrations, which if calibrated carefully with an electrometer, is on the order of $\pm 4\%$. Considering some uncertainty is also associated with the interpolated baseline values (see our response above regarding baseline correction), we believe an overall 10% uncertainty in the extinction coefficient is conservative, but reasonable.

5.) Why is particulate nitrate not considered in the NO_x/NO_y ratio? This seems odd given the authors are measuring particulate nitrate with the mAMS.

Reviewer has a great point. On average inorganic particulate nitrate was $\sim 9\%$ of total NO_y ; however, in nitrate-rich plumes, NO_3^- was a more significant fraction. We have therefore included its concentration in the NO_y budget.

The following was added to Section 2.2: “The relationship between the primary emitted nitrogen oxides (NO_x) and the higher oxidized species of nitrogen captures the transformation of NO_x in the atmosphere upon aging (Kleinman et al. 2007, Langridge et al. 2012). Thus, measurements of nitric oxide (NO), nitrogen dioxide (NO_2), nitric acid (HNO_3), particulate phase nitrate (NO_3^-) alkyl nitrates (ANs), peroxy acetyl nitrate (PAN), and peroxy propionyl nitrate (PPN) were used to calculate the ratio of primary nitrogen oxides ($\text{NO}_x = \text{NO} + \text{NO}_2$) to NO_y ($\text{NO}_y = \text{NO}_x + \text{HNO}_3 + \text{NO}_3^- + \text{ANs} + \text{PAN} + \text{PPN}$) in order to track the extent of photochemical aging in an air mass with non-zero emissions of NO_x (Kleinman et al. 2007, DeCarlo et al. 2010).”

6.) A PCASP does not seem to be the best instrument for submicron aerosol analysis. Can the authors comment on why an SMPS or UHSAS was not used in addition to the PCASP? If these instruments were not on the C-130, this needs to be stated.

Only a nano-SMPS (<100 nm) and PCASP were available among the C-130 payload. Between these two instruments, ambient measurements from PCASP were the more appropriate dataset to use since scattering efficiency for particles smaller than 100 nm at 632 nm is not significant. Additionally, even if an SMPS with a long DMA was available, the relatively long time response of the system for a full scan is not optimum for airborne characterization of pollution plumes. The following statement has been added to the manuscript in section 2.2, paragraph 6: “A Passive Cavity Aerosol Spectrometer Probe (PCASP) was available as the only instrument to measure ambient aerosol size distributions in the size range of 0.1-3 μm”. Note that the SMPS takes 60 seconds per scan, therefore is not well-suited to capture plumes of limited extent or significant spatial variation.

7.) There needs to be a discussion of the aircraft inlets and size cut points for the various instruments. This is especially critical for the PCASP vs. CAPS-PM_{ex} vs. mAMS given that the instruments have different cut points around a micron.

We have added the following sentence to section 2.2 indicating the size cut of the mAMS: “The mAMS inlet was characterized to have a 50% transmission of ~800 nm (physical diameter) particles”. In order to determine whether the discrepancy between the size ranges being sampled by the CAPS-PM_{ex} and AMS has a significant impact on our analysis or not, we have used the size distributions from the Passive Cavity Aerosol Spectrometer Probe (PCASP) instrument on board the C-130 to estimate the ambient scattering coefficients. By using a nominal refractive index of 1.5, estimated scattering (i.e., extinction, while assuming purely scattering aerosols) coefficients were calculated using the measured size distributions up to 800 nm (upper “true” size cut of the AMS) and 2000 nm (upper size cut of the inlet, and thus CAPS-PM_{ex}). The slopes of the scatter plots of the estimated scattering coefficients for PM_{0.8} vs. PM₂ under the influence of urban, O&G, agricultural, and urban+O&G slopes were 0.95 ± 0.01, 1.0 ± 0.002, and 1.0 ± 0.01, 0.92 ± 0.01, respectively, indicating that the majority of the signal contribution to extinction originated from aerosols in the size range of the mAMS. We also note that the slope values mentioned above were not highly sensitive to the choice of the refractive index. Changing the refractive index from 1.48 to 1.52 changed the slope values by at most 4%.

The following has been added to the text in section 2.2, paragraph 3 to address this issue: “Ambient aerosol size distributions were measured on-board the C-130 by a Passive Cavity Aerosol Spectrometer Probe (PCASP). Estimated extinction values using Mie calculations with a nominal refractive index of 1.5 and the measured PCASP size distributions indicated that particles smaller than 800 nm captured >92% of PM₂ extinction values, confirming that the majority of the extinction signal originated from aerosols in the size range of the mAMS. We note that the calculated extinction coefficients were not highly sensitive to the choice of refractive index; only a 4% decrease in the slope of scattering coefficients from PM_{0.8} vs. PM₂ was observed by increasing the refractive index from 1.48 to 1.52.”

8.) There needs to be a discussion of how the mAMS data was corrected for collection efficiency, especially given that agricultural plumes had significant nitrate.

Aerosol concentrations were corrected for vaporizer bounce using composition-dependent CE values. Indeed, CE in plumes heavily impacted by agricultural emissions and thus containing high levels of inorganic aerosol nitrate was higher than the nominal value (0.5).

The following sentence has been added to section 2.2 in paragraph 3 for clarification: “Aerosol concentrations from the mAMS were corrected for vaporizer bounce using composition-dependent collection efficiencies (Middlebrook 2012)”.

Comments On Results and Discussion

1.) Figure S1 appears to show roads but this is not described in the caption

Black lines on the map have been updated accordingly as interstates and highways.

2.) Again, error analysis is a problem. The uncertainty in B_{ext} being stated to be 10% when the authors state that the baseline shifts by over 5 Mm^{-1} and that the 1-sigma detection limit is 1 Mm^{-1} seems completely inconsistent. Values of B_{ext} of less than 5 Mm^{-1} are shown and the authors are suggesting the error is $< 0.5 Mm^{-1}$ for these measurements but this is half of the 1-sigma detection limit and does not account for baseline shifts. The authors make a major point that they are doing ODR because they want to weight according to the errors in the instruments, but the errors seem incorrect.

As mentioned above, majority of the baseline shifts were significantly lower than 1 Mm^{-1} . Despite that, all baseline values were interpolated for a more accurate determination of the extinction coefficient. The stated 1-s detection limit for CAPS- PM_{ex} was from one of the original papers by Massoli et al. (Massoli et al. 2012). Examining the standard deviation of the measured extinction coefficients during filtered ambient air sampling periods during the project actually indicated a lower 1-s detection limit of $\sim 1.5 Mm^{-1}$ (assuming 3- σ). Therefore we believe the uncertainty estimates used as weights of the ODR fit are reasonable. The following text in Section 2.2 has been updated to reflect the DL of this specific instrument “The estimated uncertainty in β_{ext} is 10%, while the 3- σ detection limit for 1-s data under particle free air for the conditions encountered during FRAPPE was $\sim 1.5 Mm^{-1}$ ”.

3.) Page 5 Line 17. The delta ext/co ratios have error bars associated with them, but the authors don't explain what they are. Are these 1-sigma intervals on the slope of the fitted line? For individual measurements the errors would be much larger than these ($\sim 11\%$), I am surprised at how small they are given the poor r of the fits. Also, the authors remove the error in the intercept from the discussion even though this is probably significant.

The uncertainties in the reported enhancement ratios throughout the paper represent the estimated propagated uncertainties. In Figure 2, the uncertainties are the square-root of the quadratic sum of the relative uncertainties in the ODR fit (1- σ), CO mixing ratio, and β_{ext} . The intercept and error has been added to the plots. The following has been added to Section 3.1 to clarify what the uncertainties are: “Uncertainties in the slope values of ODR fits throughout the manuscript represent the estimated propagated uncertainties, in this case, the square-root of the quadratic sum of the relative uncertainties in the ODR fit (1- σ), CO mixing ratio, and β_{ext} coefficient.”

Note also that Figure 2 is now modified to include data from the August urban plumes only. We had to remove data from July flights due to lack of optimum quantitative quality of CO data during those flights that was reflected on the data archive after the initial submission of the paper. With these changes, indeed correlation coefficients improved from $r \sim 0.6-0.7$ to $r \sim 0.85-0.9$, confirming that some species that contributed to β_{ext} were not co-emitted with CO.

4.) The authors need to explain how they arrived at the criteria of 0.7, 0.3-0.7, and < 0.3 for $NO_x:NO_y$ ratios.

Based on the comment of another reviewer, we have limited the data in Figure 2 to only those obtained in urban plumes and during August flights. With the more limited number of data points in these plumes, the aging categories are now redefined with $NO_x:NO_y > 0.5$ and < 0.5 to represent relatively fresh and aged plumes, respectively.

5.) Page 5 Line 29. The authors state that the “bulk” of the organic aerosol mass is SOA because the enhancement ratio of organic aerosol increases significantly for aged aerosol. This is not adequate reasoning. The aerosol could be unrelated to CO (from non-combustion sources), as the authors themselves point out. The increasing B_{ext} could be the result of increasing ammonium nitrate when

plumes move farther from the city. The authors need to explain what fraction of aerosol mass is accounted for by the OA:CO enhancement or something in addition to the current argument if they are going to make this sweeping statement. Also, the word “bulk” needs to be quantified in some way.

We have now limited the data in Figure 2 to those in urban plumes only. In addition, OA fraction in both fresh and aged urban plumes was ~75%; therefore, we don't expect a significant contribution from non-combustion aerosol types to β_{ext} data points in Figure 2. The following sentence has been added to Section 3.1 to clarify this: “The most dominant component of the non-refractory aerosols in urban plumes was OA, with a 74% contribution to NR-PM₁ mass. This high OA contribution combined with the observed significant increase in the enhancement ratio of OA to CO with aging (from $0.021 \pm 0.009 \mu\text{g m}^{-3} \text{ ppbv}^{-1}$ to $0.11 \pm 0.01 \mu\text{g m}^{-3} \text{ ppbv}^{-1}$) suggest that the bulk of the aged urban aerosol mass during the daytime in the Front Range was SOA. Since $\Delta\text{NO}_3^-/\Delta\text{CO}$ and $\Delta\text{SO}_4^{2-}/\Delta\text{CO}$ enhancement ratios did not increase with photochemical aging and demonstrated poor overall correlation coefficients ($r < 0.35$ for $\Delta\text{NO}_3^-/\Delta\text{CO}$ and $r < 0.29$ for $\Delta\text{SO}_4^{2-}/\Delta\text{CO}$), the increase in the enhancement ratio of aerosol optical extinction coefficient with CO was likely also driven by SOA formation.”

6.) Page 6 Line 16. Correlation coefficients of .55 are not “strong”

The sentence has now been rephrased.

7.) Page 6 Line 23. Nitric acid + aerosol nitrate is not “total” nitrate, this ignores organic nitrates.

We have clarified in the text that we refer to inorganic nitrate only since we were considering the partitioning of nitric acid between gas and aerosol phase: “In fact, the average aerosol inorganic nitrate fraction over total inorganic nitrate (aerosol nitrate/ HNO_3 + aerosol nitrate) under agriculture and O&G plumes were 0.25 ± 0.09 and 0.11 ± 0.10 , respectively, compared to 0.070 ± 0.071 in urban-influenced plumes.”

8.) The relatively weak correlations in urban plumes between Bext and any of the aerosol species (all have r less than 0.55) mass concentrations suggests that there was poor correlation between total AMS mass and Bext. In fact, this is born out in figure 4. This is very confusing and needs to be addressed, especially given the very good correlation between Bext and nitrate in agricultural plumes. The authors suggest it may be caused by a change in size distribution (Figure S2 a-b), but it appears to me that the total mass distributions in these two figures are fairly similar, even though the organic distributions are a little different. Are the authors missing an important aerosol species? Alternatively, is the mismatch in measured aerosol size between the CAPS and AMS significant (Figure S2 suggests this may be the case and that a careful application of the lens transmission is required)? If the authors are going to rest on the size-distribution argument then they need to implement a Mie model of the two distributions shown in S2 and demonstrate that they yield dramatically different Bext for the same total aerosol mass. The size distribution argument for urban + OG is more convincing.

In order to determine whether the discrepancy between the size ranges being sampled by the CAPS-PM_{ex} and AMS has a significant impact on our analysis or not, we have used the size distributions from the Passive Cavity Aerosol Spectrometer Probe (PCASP) instrument on board the C-130 to estimate the ambient scattering coefficients. By using a nominal refractive index of 1.5, estimated scattering (i.e., extinction, while assuming purely scattering aerosols) coefficients were calculated using the measured size distributions up to 800 nm (upper “true” size cut of the AMS) and 2000 nm (upper size cut of the inlet, and thus CAPS-PM_{ex}). The slopes of the scatter plots of the estimated scattering coefficients for

$PM_{0.8}$ vs. PM_2 under the influence of urban, O&G, agricultural, and urban+O&G slopes were 0.95 ± 0.01 , 1.0 ± 0.002 , and 1.0 ± 0.01 , 0.92 ± 0.01 , respectively, indicating that the majority of the signal contribution to extinction originated from aerosols in the size range of the mAMS. We also note that the slope values mentioned above were not highly sensitive to the choice of the refractive index. Changing the refractive index from 1.48 to 1.52 changed the slope values by at most 4%.

The following has been added to the text in section 2.2, paragraph 3 to address this issue: **“Ambient aerosol size distributions were measured on-board the C-130 by a Passive Cavity Aerosol Spectrometer Probe (PCASP). Estimated extinction values using Mie calculations with a nominal refractive index of 1.5 and the measured PCASP size distributions indicated that particles smaller than 800 nm captured >92% of PM_2 extinction values, confirming that the majority of the extinction signal originated from aerosols in the size range of the mAMS. We note that the calculated extinction coefficients were not highly sensitive to the choice of refractive index; only a 4% decrease in the slope of scattering coefficients from $PM_{0.8}$ vs. PM_2 was observed by increasing the refractive index from 1.48 to 1.52.”**

Upon closer examination, it became apparent that correlations between β_{ext} and neither of the non-refractory AMS species were high in the urban plumes while as shown in Figure 2, β_{ext} and CO were strongly correlated ($r > 0.85$). We suspect that BC emissions, which are indeed not included in NR- PM_1 , in urban plumes actually played an important role in controlling β_{ext} , especially in fresh plumes. It is therefore not surprising that the overall correlation of β_{ext} vs. NR- PM_1 in Figure 5a was also not high. The related paragraph in Section 3.2 is now updated to reflect these observations: **“The scatter plots of dry β_{ext} vs. OA under urban, O&G, and urban + O&G air masses presented correlation coefficients of $r = 0.46$, 0.72 , 0.46 , respectively. This observation suggests that O&G emissions are important for organic aerosol contribution to β_{ext} . On the other hand, in urban plumes, the correlation between β_{ext} and OA was lower than in O&G plumes while as demonstrated in Figure 2, β_{ext} and CO were strongly correlated under both fresh and aged air masses. These observations suggest that species other than OA, e.g., black carbon, that are co-emitted with CO are also important in driving β_{ext} in urban-influenced air masses.”** With this explanation, we have deleted sentences in Section 3.3 that emphasized the influence of size distribution shifts on MEE.

9.) In Figure 4 the removal of the intercept and its associated error is again not mentioned, even though it is a significant issue given the lines don't go through 0,0 and the r values are fairly low. I am again of the opinion that the stated error in the slopes does not accurately represent the error in this slope.

We appreciate reading reviewer's comment on the intercept in these plots.

As mentioned above, the error estimates used as weights in the ODR fits are reasonable. Figure 5 is now updated with the correct weights (taken as the standard deviation of the extinction and aerosol mass) and a more specific mask for urban-influenced plumes. With these changes, the correlation coefficients for all plume types, except urban, have improved. The low correlation of β_{ext} and NR- PM_1 mass in urban plumes is likely due to contribution of refractory BC that is not accounted for in NR- PM_1 . To further confirm this, we examined the intercept values of the ODR fits. Except for the agricultural plumes, there appears to be $\sim 2 Mm^{-1}$ of extinction when NR- PM_1 approaches 0, consistent with the hypothesis that there are some refractory components of aerosol that contribute to background extinction. Since PILS data did not indicate large concentrations of Ca^{2+} and Mg^{2+} , it's likely that this background extinction is due to background BC.

The following sentences have been added to Section 3.3 to explain the observed intercepts of the ODR fits in Figure 5: “Based on the values of the intercepts of the ODR fits in Figure 5, it appears that at background levels of NR- PM_1 mass, there was a background extinction value of $\sim 2 Mm^{-1}$ in all, except agricultural, plumes. This observation could be explained by optical extinction due to presence of refractory aerosol species, such as black carbon or dust, which are not accounted for in NR- PM_1 mass. High degree of correlation between β_{ext} and CO (Figure 2) in urban plumes and low average

concentrations of some of the dust components (e.g., calcium and magnesium) support the non-negligible contribution of BC to β_{ext} in the Front Range.”

10.) Page 8 Line 7-8. If the authors are going to make this broad conclusion they need to some basic Mie modeling to convince the reader that these shifts in size distribution can generate MEE from 1.8 to 4.1, this does not seem obvious.

After using the more specific definition of the urban plumes (defined in Section 3.1), the difference in MEE values for urban+O&G plumes vs. other plumes is not significant considering the uncertainties in the slopes of the ODR fits. We have therefore removed the reference to the importance of shifts in the size distributions and Figure 7.

11.) In Figure 7a “total mass” needs to be changed to “total non-refractory PM-1 mass”, though even the PM-1 designation is questionable with AMS data.

The reviewer is correct in mentioning that the inlet system of the AMS is not exactly a PM₁ inlet. Transmission efficiency tests of the PCI and the lens system on this specific mAMS indicated a 50% transmission of particles with physical diameter ~ 800 nm, which is comparable to other AMSs. (e.g., Bahreini et al, AST, 2008). For consistency with the common notation for AMS measurements, we have updated the label on the plot as “Total non-refractory PM₁ mass”.

12.) In Figure 7a the fit to the non-biomass burning emissions does not seem to track the data. The authors need to discuss this. Perhaps it is due to including moderate HCN data points.

We have updated this Figure to include data with masks designating the 4 plume types that have been examined in detail in the paper. This has greatly improved the correlations of β_{ext} and NR-PM₁ mass, with r values ~0.75-0.80 as well as the trends of the weighted ODR fits. Please note that because BB also contributes to atmospheric CO, we decided the conclusions drawn from the scatter plot of β_{ext} vs. CO in the presence and absence of BB could not be as robust as desired and have therefore deleted panel b.

13.) Again in Figure 7 the intercepts are removed and not discussed, they need to be discussed because they are very different between biomass burning and non-biomass burning and this has physical meaning.

Although previously the intercepts were not indicated in this figure, a discussion was provided in the text to highlight the significance of the higher intercepts observed during biomass burning days. Data in Figure 7 are now limited to those sampled in urban, urban + OG, OG, and agricultural plumes, with a more specific definition of urban plumes, and the following text in Section 3.4 has been updated accordingly: “MEE values were analyzed for days with and without the BB influence, using weighted linear ODR fit analysis, as explained previously. As seen in Figure 7, average MEE on Aug. 11-12 was ~63% greater compared to days without the influence of BB (3.65 ± 1.16 m²/g vs. 2.24 ± 0.71 m²/g). Additionally, during Aug. 11-12, background value of airborne β_{ext} was higher at 4.00 ± 0.71 Mm⁻¹ compared to 0.25 ± 0.11 Mm⁻¹ on days without the BB influence, suggesting the additional contribution to β_{ext} from the wildfires.”

References

DeCarlo, P. F., et al. (2010). "Investigation of the sources and processing of organic aerosol over the Central Mexican Plateau from aircraft measurements during MILAGRO." *Atmospheric Chemistry and Physics* **10**(12): 5257-5280.

Ely, D. W., et al. (1993). The establishment of the Denver visibility standard. Air And Waste Management Association Annual Meeting, Air And Waste Management Association. **1**.

Gilman, J. B., et al. (2013). "Source Signature of Volatile Organic Compounds from Oil and Natural Gas Operations in Northeastern Colorado." *Environmental Science & Technology* **47** 1297–1305.

Kleinman, L. I., et al. (2007). "Aircraft observations of aerosol composition and ageing in New England and Mid-Atlantic States during the summer 2002 New England Air Quality Study field campaign." *Journal of Geophysical Research-Atmospheres* **112**(D9).

Langridge, J. M., et al. (2012). "Evolution of aerosol properties impacting visibility and direct climate forcing in an ammonia-rich urban environment." *Journal of Geophysical Research: Atmospheres* **117**(D21): n/a-n/a.

Levin, E. J. T., et al. (2009). "Aerosol physical, chemical and optical properties during the Rocky Mountain Airborne Nitrogen and Sulfur study." *Atmospheric Environment* **43**(11): 1932-1939.

Massoli, P., et al. (2010). "Aerosol Light Extinction Measurements by Cavity Attenuated Phase Shift (CAPS) Spectroscopy: Laboratory Validation and Field Deployment of a Compact Aerosol Particle Extinction Monitor." *Aerosol Science and Technology* **44**(6): 428-435.

Massoli, P., et al. (2012). "Aerosol Light Extinction Measurements by Cavity Attenuated Phase Shift (CAPS) Spectroscopy: Laboratory Validation and Field Deployment of a Compact Aerosol Particle Extinction Monitor." *Aerosol Sci. Technol.* **44**: 428-435.

Middlebrook, A., et al. (2012). "Evaluation of Composition-Dependent Collection Efficiencies for the Aerodyne Aerosol Mass Spectrometer using Field Data." *Aerosol Science and Technology* **46**: 258–271.

Pétron, G., et al. (2014). "A New Look at Methane and Nonmethane Hydrocarbon Emissions from Oil and Natural Gas Operations in the Colorado Denver-Julesburg Basin." *Journal of Geophysical Research-Atmospheres* **119**(11): 6836-6852.

Petzold, A., et al. (2013). "Intercomparison of a Cavity Attenuated Phase Shift-based extinction monitor (CAPS PMex) with an integrating nephelometer and a filter-based absorption monitor." *Atmospheric Measurement Techniques* **6**(5): 1141-1151.

Scamehorn, H. L. (2002). *High Altitude Energy: A History of Fossil Fuels in Colorado*. Boulder, CO. Colorado, University Press of Colorado.

Watson, J. G., et al. (1998). *Northern Front Range Air Quality Study Final Report*, Colorado State University.

Aerosol Optical Extinction during the Front Range Air Pollution and Photochemistry Experiment (FRAPPÉ) 2014 Summertime Field Campaign, Colorado U.S.A.

Justin H. Dingle¹, Kennedy Vu¹, Roya Bahreini^{1,2}, Eric C. Apel³, Teresa L. Campos³, Frank Flocke³, Alan Fried⁴, Scott Herndon⁵, Alan J. Hills³, Rebecca S. Hornbrook³, Greg Huey⁶, Lisa Kaser³, Denise D. Montzka³, John B. Nowak⁵, Mike Reeves³, Dirk Richter⁴, Joseph R. Roscioli⁵, Stephen Shertz³, Meghan Stell³, David Tanner⁶, Geoff Tyndall³, James Walega⁴, Petter Weibring⁴, Andrew Weinheimer³

¹ Environmental Toxicology Graduate Program, University of California, Riverside, CA 92521

² Department of Environmental Sciences, University of California, Riverside, CA 92521

³ National Center for Atmospheric Research, Boulder, CO 80301

⁴ Institute for Arctic and Alpine Research, University of Colorado, Boulder, CO 80303

⁵ Aerodyne Research, Inc., Billerica, MA 01821

⁶ Department of Earth and Atmospheric Sciences, Georgia Institute of Technology, Atlanta, GA 30033

Corresponding author: R. Bahreini (roya.bahreini@ucr.edu)

Abstract. Summertime aerosol optical extinction (β_{ext}) was measured in the Colorado Front Range and Denver Metropolitan Area as part of the Front Range Air Pollution and Photochemistry Experiment (FRAPPÉ) campaign during July-August 2014. An Aerodyne Cavity Attenuated Phase Shift particle light extinction monitor (CAPS-PM_{ex}) was deployed to measure ~~dry~~- β_{ext} (at average relative humidity of 20 ± 7%) -of submicron aerosols at $\lambda=632$ nm at 1 Hz. Data from a suite of gas-phase instrumentation were used to interpret β_{ext} behavior under various categories of air masses and sources. Extinction enhancement ratios relative to CO ($\Delta\beta_{\text{ext}}/\Delta\text{CO}$) were ~~significantly increased higher~~ in ~~highly~~-aged urban air masses compared to fresh air masses by ~~~50-60%~~. The resulting increase in $\Delta\beta_{\text{ext}}/\Delta\text{CO}$ under highly aged air masses was accompanied by formation of secondary organic aerosols (SOA). In addition, the impacts of aerosol composition on β_{ext} in air masses under the influence of urban, natural oil and gas operations (O&G), and agriculture and livestock operations were evaluated. Estimated non-refractory mass extinction efficiency (MEE) values for different air mass types ranged from ~~1.51-2.274.83-3.30~~-m² g⁻¹, with the minimum and maximum values observed in urban and agriculture ~~and urban + O&G~~ influenced air masses, respectively. The mass distribution for organic, nitrate, and sulfate aerosols presented distinct profiles in different air mass types. During Aug. 11-12, regional influence of a biomass burning event was observed, increasing the background β_{ext} ~~and by 10-154 Mm⁻¹ and the~~ estimated MEE ~~and $\Delta\beta_{\text{ext}}/\Delta\text{CO}$~~ -values in the Front Range.

1 Introduction

Aerosol optical extinction coefficient (β_{ext}) represents the attenuation of light due to aerosol absorption and scattering of solar radiation. For a population of aerosol particles, β_{ext} depends on aerosol size, composition, particle number concentration, shape and morphology (Bohren et al. 1998). Atmospheric aerosols have important implications on climate. They modify the Earth's radiative energy budget directly through absorption and scattering of light, and indirectly through changing cloud characteristics (e.g., cloud droplet number concentration, cloud droplet size, cloud reflectivity, or lifetime) (Ramanathan et al. 2001, Seinfeld et al. 2006, Langridge et al. 2011). In addition, aerosols with diameters between 0.1 μm to 1 μm are the main contributors to visibility degradation in anthropogenically polluted areas and on regional scales due to their direct interactions with solar radiation (Malm 1989, Hobbs 2000, Ying et al. 2004). For example, it has been observed that the important anthropogenic contributors to light scattering in the Colorado Rocky Mountains are particulate matter from the urban emissions (Levin et al. 2009). The Denver Metropolitan area has also experienced seasonal air pollution and visibility degradation in the past. The wintertime pollution in Denver when trapped closer to the surface due to the low inversion layer causes a greyish-brown cloud referenced to as "Denver Brown Cloud." The composition of the Denver Brown Cloud and contribution of different chemical species to the observed β_{ext} during the wintertime have been investigated in 1970's to late 1980's (Groblicki et al. 1981, Wolff et al. 1981, Neff 1997). These studies concluded that among all the measured aerosol species, elemental carbon, ammonium sulfate, and ammonium nitrate contributed the most (37.7%, 20.2%, and 17.2 %, respectively) to wintertime optical extinction in the visible range. Previous measurements of summertime particle composition in the Colorado Front Range were conducted during the Northern Front Range Air Quality Study (NFRAQS) between July 17 to August 31, 1996 at several urban and rural sites. The major components of $\text{PM}_{2.5}$ mass were identified to be carbonaceous and inorganic aerosols, with carbonaceous aerosols contributing to about 46% of $\text{PM}_{2.5}$ mass. The 24-hour average measurements of $\text{PM}_{2.5}$ organic carbon, nitrate, and sulfate particles were observed to be 4.2 $\mu\text{g}/\text{m}^3$, 0.9-1.2 $\mu\text{g}/\text{m}^3$, and 1.4-1.5 $\mu\text{g}/\text{m}^3$, respectively (Watson et al. 1998) (Watson et al 1998). In response to the wintertime haze episodes observed in the region, the State of Colorado has implemented a visibility standard based on total optical extinction of 76 Mm^{-1} at 550 nm, averaged during a 4-hr period when ambient RH is less than 70% (Ely et al. 1993). Total optical extinction measurements are provided by the Colorado Department of Public Health and Environment's transmissometer installed in Downtown Denver. The average total extinction values of August 2001-2014, ranging from 40-80 Mm^{-1} , reveal no significant trend in summertime extinction and visibility in the region since 2001. Despite the extensive studies of the Denver Brown Cloud in 1970s and 1980s, recent comprehensive summertime characterization of air quality in the Colorado Front Range has been lacking.

The meteorological influence on air quality and visibility in the Front Range can also be important (e.g., Vu et al. 2016). Typically during the day, easterly upslope flow transports emissions from local sources westward while during the night, the flow reverses and downslope drainage flow through Platte River Valley sets in. Occasionally, a synoptic scale cyclone, called the Denver Cyclone, is established when drainage flow of air masses is prevented due to propagation of a

vortex that develops east of the Rocky Mountains, contributing to transport and mixing of air masses in a cyclonic flow pattern (Crook et al. 1990, Reddy et al. 1995).

With a twofold increase in natural resource extraction wells since 2005 to about 24,000 active oil and natural gas (O&G) production wells in 2012, northeastern Colorado has experienced extensive fossil fuel production within the past decade (Scamehorn 2002, Pétron et al. 2014). This includes increases in fossil fuel production from coal bed methane, tight sand and shale natural gas, shale oil, and the associated gases. The emissions from these processes have several environmental impacts such as greenhouse emissions of methane and emissions of non-methane hydrocarbons that impairs air quality. Emissions from diesel trucks, drilling rigs, power generators, phase separators, dehydrators, storage tanks, compressors and pipes used in O&G operations also contribute to the regional burden of volatile organic compounds (VOCs), nitrogen oxides, and particulate matter (i.e., black carbon and primary organic carbon) (Gilman et al. 2013). One of the major air quality issues the Colorado Front Range faces is the exceedance of the 8-hour National Ambient Air Quality Standard (NAAQS) standard for ozone (75 ppbv) during the summertime. In 2007, the Denver metropolitan area and the northern parts of the Colorado Front Range were classified as nonattainment areas due to the summertime elevated levels of ozone (www.colorado.gov/cdphe/attainment). ~~In the wintertime, it has been estimated that ~55% of the VOC-OH reactivity was attributed to O&G operations, indicating that photochemical production of ozone is significantly impacted by O&G emissions (Gilman et al. 2013).~~ Summertime impacts of such O&G emissions on the formation of secondary pollutants and visibility reduction in the Front Range have not been explored previously. In addition to local point and area sources in the Front Range, biomass burning emissions from wildfires in the region may also act as a source of aerosols, contributing to regional haze (Park et al. 2003).

During July-August 2014, airborne measurements were conducted over the Colorado Front Range as part of the Front Range Air Pollution and Photochemistry Experiment (FRAPPÉ) to characterize the influence of sources, photochemical processing, and transport on atmospheric gaseous and aerosol pollutants in the area. This paper will discuss the role of local aerosol sources in the Front Range and regional wildfires on aerosol optical extinction in the absence of the Denver Cyclone by investigating chemical and optical properties of aerosols in different air masses.

2 Measurements

2.1 FRAPPÉ Field Campaign

In-situ measurements were conducted aboard the National Science Foundation/National Center for Atmospheric Research (NSF/NCAR) C-130 aircraft during July 20-August 18, 2014. Flight tracks of the C-130, color coded with different trace gases, are presented in Figure 1a-c. In the current analysis, airborne data were limited to those obtained during August and only in the boundary layer of the Colorado Front Range (i.e., altitudes below 2500 m above sea level (ASL) east of the foothills and below 5500 m ASL with easterly winds over the foothills and the Continental Divide) to capture the influence of local sources such as power plants, O&G, agriculture, livestock, and urban emissions. Occasionally, when air masses with

the mountain-valley circulation patterns were sampled, data from higher altitudes (< 4000 m ASL) over the Denver Metropolitan area were also considered.

2.2 Instrumentation and Methodology

The NSF/NCAR C-130 aircraft carried an extensive collection of instruments for the characterization of the diverse atmospheric pollutants in the Colorado Front Range. The relevant instrumentations used in the current analysis are described below. (The data produced by these instruments are available at <http://www-air.larc.nasa.gov/cgi-bin/ArcView/discover-aq.co-2014?C130=1>).

The parameter extinction coefficient (β_{ext}) at 632 nm was measured using a Cavity Attenuated Phase Shift particle light extinction monitor (CAPS-PM_{ex}) (Aerodyne Research Inc., Billerica, MA). The CAPS-PM_{ex} utilizes high reflectivity mirrors at two ends of a 26-cm long, near-confocal cavity. Within the optical cell cavity, the highly reflective mirrors create an effective path length of approximately 2 km. Under the particle free sampling mode, the light emitting diode (LED) light output is directed to the first mirror, then while a small fraction goes passes through the second mirror to the photodiode detector, producing a slightly distorted waveform of the square-wave modulated by the LED, whereas under the aerosol sampling mode, the detector detects a greater distorted waveform, characterized by a phase shift. The vacuum photodiode, which is located behind the second reflective mirror detects and measures that phase shift when the square wave becomes distorted due to the interactions with sampled air under a relatively long effective pathlength. The observed phase shift is then related to aerosol β_{ext} as follows:

$$\beta_{ext} = (\cot\theta - \cot\theta_0) * (2\pi f/c), \quad (1)$$

where $\cot\theta_0$ is the phase shift from the particle-free sampling mode, $\cot\theta$ is the phase shift during the aerosol sampling mode, f is the frequency, and c is the speed of light. The estimated uncertainty in β_{ext} is 10%, while the 3- σ detection limit for 1-s data under particle free air for the conditions encountered during FRAPPE was was is s 3~1.5 Mm⁻¹ (Massoli et al. 2010, Petzold et al. 2013). Measurements of the baseline were conducted through the system's internal filter unit regularly, at 5 minute intervals. The filter period, which lasted for 1 minute, included 10 s of flush time, 40 s of filter sampling, followed by another 10 s of flush time. Although for majority (72%) of the data, consecutive baseline values had shifted by less than 0.5 Mm⁻¹, -baseline values were interpolated for a more accurate estimation of optical extinction. CAPS-PM_{ex} data, obtained at 1 Hz, were averaged to aerosol mass spectrometer's averaging time of 15 s. -The measured β_{ext} includes the combined effects of scattering and absorption of light by aerosols at 632 nm; given relatively high single scattering albedo values of aerosols downwind of urban environments (Langridge et al. 2012), β_{ext} is expected to be dominated by scattering coefficient. As discussed in Section 3.3 and 3.4, in urban- or biomass burning-influenced air masses, contribution of absorption by black carbon to β_{ext} could be more significant. It is worth mentioning that anthropogenic gases such as nitrogen dioxide have minimal effect on the measured β_{ext} at 632 nm since regular baseline corrections based on sampled filtered air were applied

to the data. Given the average mixing ratio of NO_2 , the parameterization by Groblicki et al. (1981) for estimating NO_2 absorption at 550 nm, and the factor of 10 smaller value of NO_2 absorption cross section at 632 nm compared to 550 nm (Schneider et al. 1987), we estimated the average contribution of NO_2 absorption at 632 nm to be $\sim 0.1 \text{ Mm}^{-1}$, indicating a minor contribution to total extinction at 632 nm.

The CAPS- PM_{ex} shared a common inlet with a compact Aerosol Mass Spectrometer (mAMS; Aerodyne Inc., Billerica, MA) coupled with a time-of-flight (TOFwerk, Thun, Switzerland) detector to measure particle mass distribution and non-refractory submicron aerosol composition (NR- PM_1) of organics, nitrate, sulfate, chloride, and ammonium. The mAMS inlet was characterized to have a 50% transmission of $\sim 800 \text{ nm}$ (physical diameter) particles. Aerosol concentrations from the mAMS were corrected for vaporizer bounce using composition-dependent collection efficiencies (Middlebrook et al. 2012). The estimated uncertainty for all aerosol species is $\sim 30\%$ (Bahreini et al. 2009). Both instruments sampled particles through a secondary diffuser mounted inside a NCAR HIAPER modular inlet (HIMIL), mounted facing forward, under the C-130 aircraft. Given the total flow rate within the inlet and assuming particle density of 1500 kg/m^3 , ambient temperature of $20 \text{ }^\circ\text{C}$, and ambient pressure of 70 KPa, $2 \text{ }\mu\text{m}$ particles were estimated to be transmitted by 50%, making the inlet nominally a PM_2 inlet. Residence time in the inlet was estimated to be $\sim 0.56 \text{ s}$. The CAPS PM_{ex} was set to measure at 1 Hz frequency. Ambient aerosol size distributions were measured on-board the C-130 by a Passive Cavity Aerosol Spectrometer Probe (PCASP). Estimated extinction values using Mie calculations with a nominal refractive index of 1.5 and the measured PCASP size distributions indicated that particles smaller than 800 nm captured $>92\%$ of PM_2 extinction values, confirming that the majority of the extinction signal originated from aerosols in the size range of the mAMS. We note that the calculated extinction coefficients were not highly sensitive to the choice of refractive index; only a 4% decrease in the slope of scattering from $\text{PM}_{0.8}$ vs. PM_2 was observed by increasing the refractive index from 1.48 to 1.52.

Based on the ambient relative humidity (RH) and temperature and the temperature within the CAPS- PM_{ex} extinction cell, and assuming that aerosols had equilibrated to the conditions within the measurement cell, the CAPS- PM_{ex} measurements for during the flights discussed here represent extinction values at an average RH of $20 \pm 7\%$ (range of 15-30%). Additionally, β_{ext} values were normalized for STP (273 K and 1 atm) conditions. It is worth reiterating that have minimal since regular baseline corrections based on sampled filtered air were applied to the data. Given taverage mixing ratio of NO_2 , the parameterization by Groblicki et al. (1981) for estimating NO_2 absorption at 550 nm, and the factor of 10 smaller value of NO_2 absorption cross section at 632 nm compared to 550 nm (Schneider et al. 1987), we the average absorption of NO_2 to be ~ 0.1 , indicating a minor contribution of NO_2 to total extinction at 632 nm.

The relationship between the primary emitted nitrogen oxides (NO_x) and the higher oxidized species of nitrogen intends to captures the transformation of NO_x in the atmosphere upon aging (Kleinman et al. 2007, Langridge et al. 2012). Thus, measurements of nitric oxide (NO), nitrogen dioxide (NO_2), nitric acid (HNO_3), particulate phase nitrate (NO_3^-), alkyl nitrates (ANs), peroxy acetyl nitrate (PAN), and peroxy propionyl nitrate (PPN) were used to calculate the ratio of primary nitrogen oxides ($\text{NO}_x = \text{NO} + \text{NO}_2$) to NO_y ($\text{NO}_y = \text{NO}_x + \text{HNO}_3 + \text{NO}_3^- + \text{ANs} + \text{PAN} + \text{PPN}$) in order to track the extent of photochemical aging in an air mass with non-zero emissions of NO_x (Kleinman et al. 2007, DeCarlo et al. 2010). A ratio that

yields a value close to one represents air masses that are relatively fresh whereas a ratio closer to zero represents more aged air mass. NO and NO₂ were measured using the NCAR 2-channel chemiluminescence instrument (Ridley et al. 1990). A chemical ionization mass spectrometer (CIMS) coupled with a quadrupole detector was operated to measure HNO₃, using SF₅⁻ as the reagent ion (Huey et al. 1998, Huey 2007). ANs were measured using thermal dissociation-laser induced fluorescence (TD-LIF) (Thornton et al. 2000, Day et al. 2002). PAN and PPN species were measured using the NCAR PAN-CIGAR CIMS (Slusher et al. 2004, Zheng et al. 2011), with I⁻ as the reagent ion.

The impacts of different pollution sources on sampled air masses were characterized by considering several auxiliary gas-phase tracers. Carbon monoxide, the tracer for combustion emissions, was measured by VUV-fluorescence with the estimated uncertainty of 3% (Gerbig et al. 1999). Ethane (C₂H₆), used to identify influence of O&G emissions, was measured using the Compact Atmospheric Multi-species Spectrometer (CAMS), employing infrared spectrometry (Richter et al. 2015). The Aerodyne dual quantum cascade trace gas monitor for ammonia (NH₃) equipped with a mid-infrared absorption spectrometer was used to identify emissions of agriculture and livestock operations (Ellis et al. 2010). The influence of biomass burning was identified using the measurements of hydrogen cyanide from the NCAR Trace Organic Gas Analyzer (TOGA), a fast gas chromatography coupled with a quadrupole mass spectrometer (GC-MS) set to selected ion monitoring mode for quantification (Apel et al. 2015) and acetonitrile by proton-transfer reaction mass spectrometry (PTR-MS), a high sensitivity instrument with fast time response that employs a quadrupole mass spectrometer to measure volatile organic compounds (de Gouw et al. 2007, Karl et al. 2009). A Passive Cavity Aerosol Spectrometer Probe (PCASP) ~~was available; as the only~~ instrument ~~which to~~ measure ~~ambient~~ aerosol size distributions ~~under ambient conditions~~ in the size range of 0.1-3 μm, ~~was utilized to determine the particle number concentrations under different sources or air mass types as described above~~ (Rosenberg et al. 2012).

3. Results and Discussion

3.1 ~~Aerosol~~ Urban Aerosol optical extinction characterization under different photochemical aging regimes

NO_x/NO_y ratios were observed to be highest over the city representing freshly emitted plumes from vehicular traffic (Figure S1). Away from the city center, NO_x/NO_y values decrease, representing the relative evolution of fresh air masses containing NO_x. Figure 2 shows the scatter plot of β_{ext} vs. CO, color coded with the NO_x/NO_y ratio, on ~~July 26, 29, 31 and~~ August 2-3, 7-8, 15-16, 18 (i.e., excluding days with the influences of the Denver Cyclone and biomass burning events). Measurements here focused on air masses impacted by urban sources only, as defined by enhancement of CO over the background (105 ppbv, as defined by the mode in the frequency distribution of CO in the Front Range boundary layer) while ΔC₂H₆/ΔCO < 20 pptv ppbv⁻¹ (Warneke et al. 2007, Borbon et al. 2013). The extinction enhancement ratios Δβ_{ext}/ΔCO under 2-3-aging regimes, categorized by NO_x/NO_y ratio values, were analyzed by weighted linear orthogonal distance regression (ODR) fits, with the slopes representing the enhancement ratios. In obtaining these fits, weights represented standard deviations equal to the uncertainties in CO (3%) and β_{ext} (10%). Uncertainties in the slope values of ODR fits throughout the manuscript

represent the estimated propagated uncertainties, in this case: e , the square-root of the quadratic sum of the relative uncertainties in the ODR fit ($1-\sigma$), CO mixing ratio, and β_{ext} coefficient. NO_x/NO_y values of <0.53 , $0.3-0.7$, and >0.57 represent relatively aged, intermediately aged, and fresh NO_x -containing air masses, respectively. Measurements here focused on air masses impacted by only, as defined by enhancement of CO over the background (105 ppbv , as defined by the mode in the frequency distribution of CO in the Front Range boundary layer) while $\Delta\text{C}_2\text{H}_6/\Delta\text{CO} < 20 \text{ pptv ppbv}^{-1}$. Different trends in $\Delta\beta_{\text{ext}}/\Delta\text{CO}$ were seen under the ~~two~~three aging regimes, with ~~the a lowest lower~~ values of $0.1346 \pm 0.01405 \text{ Mm}^{-1} \text{ ppbv}^{-1}$ and $0.15 \pm 0.004 \text{ Mm}^{-1} \text{ ppbv}^{-1}$ observed in the fresh and intermediately aged air masses, respectively. On the other hand, the most relatively aged air masses showed ~~the a highest higher~~ $\Delta\beta_{\text{ext}}/\Delta\text{CO}$ value of $0.2025 \pm 0.025004 \text{ Mm}^{-1} \text{ ppbv}^{-1}$, indicating about a 540% factor of -21.6 increase in the extinction enhancement ratio due to photochemical aging. The correlation coefficient r values were 0.9263 , 0.73 , and 0.64 and 0.85 for relatively fresh, intermediately aged and aged air masses, respectively. Note that the NO_x/NO_y photochemical clock provides a true measure of atmospheric processing only for air masses influenced by emissions from high temperature combustion processes, e.g., on road or off road vehicular exhaust. Therefore, age classification based on the NO_x/NO_y value does not differentiate between a purely combustion-derived air mass with a certain photochemical age and the same air mass mixed with a fresh or aged plume from non-combustion sources. Therefore, it is possible that the plumes categorized with a given NO_x/NO_y value were non-uniformly mixed with differently aged, non-combustion-influenced air masses, resulting in a lower than optimum correlation coefficients in Figure 2. Similarly, a photochemical clock based on the ratios of different VOCs does not provide an accurate estimate of plume processing times in this environment due to different emission ratios of most VOCs from urban and O&G sources. Regardless of this caveat, The most dominant component of the non-refractory aerosols in urban plumes was OA, with a 74% contribution to NR-PM₁ mass. The high OA contribution combined with the observed significant increase in the enhancement ratio of OA to CO with aging (from $0.021 \pm 0.009 \mu\text{g m}^{-3} \text{ ppbv}^{-1}$ to $0.11 \pm 0.01 \mu\text{g m}^{-3} \text{ ppbv}^{-1}$) suggest that the bulk of the organic aerosol aged urban aerosol mass during the daytime in the Front Range was characterized as SOA, due to the observed significant increase in the enhancement ratio of OA to CO with aging: $\Delta\text{OA}/\Delta\text{CO}$ was a factor of -63 higher in air masses with $\text{NO}_x/\text{NO}_y < 0.53$ ($0.19073 \pm 0.16002 \mu\text{g m}^{-3} \text{ ppbv}^{-1}$, $r=0.6076$) compared to those with $\text{NO}_x/\text{NO}_y > 0.57$ ($0.0297 \pm 0.01304 \mu\text{g m}^{-3} \text{ ppbv}^{-1}$, $r=0.7467$). However, since the $\Delta\text{NO}_3/\Delta\text{CO}$ and $\Delta\text{SO}_4^{2-}/\Delta\text{CO}$ enhancement ratios did not increase with photochemical aging and demonstrated poor overall correlation coefficients ($r < 0.3527$ for $\Delta\text{NO}_3/\Delta\text{CO}$ and $r < 0.2949$ for $\Delta\text{SO}_4^{2-}/\Delta\text{CO}$), therefore, the increase in the enhancement ratio of aerosol optical extinction coefficient with CO was likely also driven by SOA formation.

3.2 Impacts of source and aerosol composition on aerosol optical extinction

Analysis of the average composition of NR-PM₁ in the Northern Front Range, in the absence of the Denver Cyclone, revealed significantly higher concentrations of organic aerosols relative to inorganic anions in the urban- and urban + O&G-influenced air masses, with a fractional contribution of $\sim 74\%$ (Figure 3). In O&G and agriculturally influenced air masses,

organic fraction was lower, at 65% and 57%, respectively. On average, similar concentrations of non-refractory aerosol sulfate and chloride were observed in the different air masses while concentration of nitrate aerosols increased by a factor of ~2-3 in agriculturally-influenced air masses compared to the other air mass types with the exception of urban+O&G air masses.

5 Aerosol optical extinction values under the influence of different sources were further analyzed using auxiliary gas-phase data. ~~CO, C₂H₆, and NH₃ tracers represent urban emissions, O&G, and agricultural and livestock operations, respectively. As mentioned in Section 3.1., u~~Urban emissions were classified by enhancement of CO over the background (105 ppbv, as defined by the mode in the frequency distribution of CO in the Front Range boundary layer) while $\Delta C_2H_6/\Delta CO < 20$ pptv ppbv⁻¹ with enhancement in CO relative to the background (95-105 ppbv), while, O&G and agricultural emissions were classified using enhancements of C₂H₆ over 2500 pptv, and that of ammonia over 5 ppbv, respectively, when all other tracers were at background level. A fourth air mass classification used in this analysis, urban + O&G, ~~is the combination of the urban and~~ is based on O&G air masses when where both CO and C₂H₆ mixing ratios were elevated above the background ~~urban and O&G classifications were satisfied.~~ The background mixing ratios for each gas tracer were determined by the mode of the frequency distribution of the tracer's mixing ratio observed in each flight. The impacts of sources and aerosol composition on extinction were explored by considering correlation coefficients of linear least-squared regression fits to the scatter plots of aerosol extinction vs. the mass concentration of the three dominant aerosol species (OA, nitrate aerosols, and sulfate aerosols) in urban-, O&G-, urban + O&G, and agricultural-influenced air masses.

Figure 4 shows the correlation coefficient (r) values of ~~dry~~ extinction vs. aerosol species mass concentration, in different air mass types as characterized above. The ~~relationship between~~ scatter plots of dry β_{ext} vs. OA revealed a strong positive correlation under urban, O&G, and urban + O&G air masses presented correlation coefficients of (r = 0.5546, 0.7472, 0.5546, respectively). This observation suggests that O&G emissions are important for organic aerosol contribution to β_{ext} . On the other hand, in urban plumes, the correlation between β_{ext} and OA was lower than in O&G plumes while as demonstrated in Figure 2, β_{ext} and CO were strongly correlated under both fresh and aged air masses. These observations suggest that species other than OA, e.g., black carbon, that are co-emitted with CO are also important in driving β_{ext} in urban- influenced air masses. ~~This observation, combined with the evolution of $\Delta\beta_{ext}/\Delta CO$ upon aging, suggests that organic aerosols are a critical component of PM in driving β_{ext} in the Colorado Front Range. However the~~ The correlation between ~~dry~~ β_{ext} vs. OA was weakest in plumes with agricultural emissions (r = 0.0850-17), suggesting OA had little impact on β_{ext} in these plumes. The correlation coefficients for β_{ext} vs. aerosol nitrate mass were strongest under the influence of O&G, urban+ O&G, and agriculture and livestock emissions (r = 0.74-75, 0.75 and 0.90 respectively), and weakest in the urban plumes (r = 0.180-37). Aerosol nitrate formation depends on ambient conditions (temperature and relative humidity), relative mixing ratios of nitric acid and ammonia, as well as aerosol composition and pH (Seinfeld et al. 2006, Weber et al. 2016). With uniform concentrations of sulfate aerosol and small contribution of chloride and dust components to the Front Range fine aerosol mass, variability in aerosol pH variability of the particles was not expected to be high. Furthermore, there was no specific trend in temperature or relative humidity in different plume types. On the other hand, mixing ratios of ammonia

were observed to be variable in the different air masses, with average values of 1.41 ± 1.2 ppbv, 2.75 ± 1.88 ppbv, 8.21 ± 2.06 ppbv, and 5.47 ± 1.81 ppbv in urban, O&G, agriculture, and urban+O&G plumes, respectively. These observations suggest that ammonia emissions that are co-located with O&G-related activities in the Front Range play a significant role in controlling β_{ext} in these air masses by enhancing the partitioning of nitric acid to the condensed phase. In fact, the average aerosol inorganic nitrate fraction over total inorganic nitrate (aerosol nitrate/ [HNO₃ + aerosol nitrate]) under agriculture and O&G plumes were 0.25 ± 0.09 and 0.11 ± 0.10 , respectively, compared to 0.070 ± 0.071 in urban-influenced plumes. β_{ext} was poorly correlated with sulfate aerosols in the region under the influence from all sources ($r = 0.2730, 0.3337, 0.07, 0.0823$ for urban, O&G, agriculture, and urban+O&G respectively), suggesting a low impact of sulfate aerosol and its precursors on ~~dry~~ β_{ext} in the region.

Due to the higher hygroscopicity of inorganic salts compared to organics, contribution of sulfate and nitrate aerosols to the ambient β_{ext} could be higher than what is discussed above. However, under the average ambient conditions encountered during FRAPPÉ (average RH $\sim 44 \pm 17$ %), the increase in ambient β_{ext} due to aerosol hygroscopicity is not expected to be significant ($\sim 20\%$) given the high organic fraction of 64-74% in urban-, O&G-, or urban + O&G-influenced plumes (Massoli et al. 2009). In agriculturally-influenced plumes, the influence of nitrate aerosol on ambient β_{ext} will be greater because of the lower organic fraction and higher nitrate mass in these plumes, re-emphasizing the role of nitrate aerosol on β_{ext} under such emissions.

3.3 Mass Extinction Efficiency

Mass extinction efficiency (MEE) is a function of the diameter of the particle, wavelength of attenuated light, and aerosol refractive index (Seinfeld et al. 2006). To further assess the impacts of aerosol sources on ~~dry~~ β_{ext} , MEE values, i.e., the ratio of the observed ~~dry~~ β_{ext} to NR-PM₁ mass, in different air masses were estimated. For this analysis, MEE values were determined as the slope of the weighted linear ODR fits of β_{ext} against NR-PM₁ mass, with weights representing standard deviations equal to the uncertainties in NR-PM₁ mass (30%) and β_{ext} (10%). As indicated in Figure 5a-d, MEE values under the urban, O&G, agriculture, and urban + O&G influence were $\sim 1.97 \pm 1.51 \pm 0.49084 \text{ m}^2 \text{ g}^{-1}$ ($r=0.40$), $1.6288 \pm 0.51064 \text{ m}^2 \text{ g}^{-1}$ ($r=0.79$), $2.27483 \pm 0.838 \text{ m}^2 \text{ g}^{-1}$ ($r=0.83$), and $2.14330 \pm 0.68094 \text{ m}^2 \text{ g}^{-1}$ ($r=0.73$) with r values of 0.52, 0.78, 0.79, and 0.59, respectively. The highest average MEE value was observed in agricultural urban + O&G plumes although considering the uncertainties in the fitted slopes, the MEE values were not significantly different. The overall MEE value in the Front Range, i.e., MEE observed for aerosols in all air mass types, but in the absence of biomass burning, was $2.2466 \pm 0.71024 \text{ m}^2 \text{ g}^{-1}$ ($r = 0.8074$). Based on the values of the intercepts of the ODR fits in Figure 5, it appears that at background levels of NR-PM₁ mass, there was a background extinction value of $\sim 2 \text{ Mm}^{-1}$ in all, except agricultural, plumes. This observation could be explained by optical extinction due to presence of refractory aerosol species, such as black carbon or dust, which are not accounted for in NR-PM₁ mass. High degree of correlation between β_{ext} and CO (Figure 2) in urban plumes and low average concentrations of some of the dust components (e.g., calcium and magnesium) throughout the region support the non-negligible contribution of BC to β_{ext} in the Front Range.

As seen in Figure S2, different aerosol mass distributions were observed under different air mass types. For the mass distribution analysis, d_{va} (vacuum aerodynamic diameter) was converted to d_p (physical diameter) by dividing d_{va} by the overall mass-weighted effective density (ρ), assuming $\rho=1.25 \text{ g cm}^{-3}$ for OA, $\rho =1.75 \text{ g cm}^{-3}$ for ammonium sulfate and ammonium nitrate, and assuming that particles sampled by the mAMS were internally mixed (Jayne et al. 2000, Seinfeld et al. 2006).

For typical urban air masses, ~~with data points along the line of the ODR fit of Figure 5a~~ mass distributions were dominated by organic aerosols in the size range of $d_p=150\text{-}300\text{-}500 \text{ nm}$ (Figure S3S2a). This is consistent with previous observations for urban aerosol volume distributions with modes at the size range of $d_p \sim 200\text{-}500 \text{ nm}$ (Seinfeld et al. 2006). ~~To investigate the reason behind the low r value for the observations under the urban influence, data points below and above the ODR fit of Figure 5a were analyzed. Different mass distributions were observed for points below and above the ODR fits (Figure S2 a b). A mode of $\sim 200\text{-}250 \text{ nm}$ was seen for both sets of data while a second mode at $\sim 400 \text{ nm}$ was also observed for points above the ODR fit. Differences in the size distributions of urban aerosols might have contributed to the spread in the scatter plot and hence the lower r value in Figure 5a.~~ Under O&G air masses (Figure S2eS2b), individual mass distributions were broader, with modes for all species shifted to larger sizes ($d_p \sim 200\text{-}550 \text{ nm}$). In agriculturally-influenced air masses nitrate aerosols presented a significant mode in the size range of $d_p \sim 250\text{-}400 \text{ nm}$ while OA species were concentrated on smaller sizes ($d_p \sim 100\text{-}200 \text{ nm}$; Figure S2dS2c).

~~As mentioned above, the average MEE value in the urban + O&G plumes was significantly on average higher than in the other air masses although not significantly. Mass distributions with different MEE values, i.e., in plumes with data points below the ODR fit, $MEE=1.83 \pm 0.80 \text{ m}^2 \text{ g}^{-1}$, and above the ODR fit, $MEE=4.12 \pm 0.69 \text{ m}^2 \text{ g}^{-1}$ (Figure S4) were examined. Similar to the urban mass distributions discussed above, the~~ The mass distributions in urban + O&G plumes were more variable. Occasionally, the distribution was dominated by OA in the smaller size range ($\sim 90\text{-}110 \text{ nm}$), but it also included contributions from sulfates and nitrates in the larger size ($\sim 225\text{-}275 \text{ nm}$ and $\sim 430\text{-}550 \text{ nm}$) (Figure S2d) while other times the mass distribution had significantly higher contribution from OA in the size range of $\sim 225\text{-}350 \text{ nm}$, showing a clear shift and OA growth to larger sizes (Figure S2e). ~~To gain a more comprehensive understanding of the impacts of variable size distributions on β_{ext} and MEE values, PCASP number concentrations in the size range of $300\text{-}2000 \text{ nm}$ ($N_{300\text{-}2000}$), where Q_{SP} is more significant, were further examined. As shown in Figure 6 (also Figure S5), 60-90% of data obtained under the urban, O&G, and agriculture air masses, contained less than 15 particle/cm^3 in the size range of $300\text{-}2000 \text{ nm}$. This consistent observation of low number concentration in $N_{300\text{-}2000}$ supports the similarity of the low MEE values in these air masses. In contrast, 55-90% of data under the influence of urban+O&G mixed emissions, especially those with extinction values higher than the ODR fit, contained $N_{300\text{-}1000}$ more than 15 particle/cm^3 . Higher contribution of larger particles in the urban+O&G mixed air masses is consistent with the higher average MEE value observed in these air masses (Figure 5d). It is worth noting that the PCASP data were obtained at ambient conditions whereas the aerosol sampled by CAPS PM_{ex} and AMS were effectively dried upon sampling in the cabin at lower RH ($\sim 15\text{-}30\%$). Therefore, the ambient size range of $300\text{-}2000 \text{ nm}$ might translate to a slightly different dry size range due to day to day changes in the ambient relative humidity (RH)RH and~~

~~variable aerosol hygroscopicity. However, this influence is expected to be minimal since average ambient RH levels were relatively low (~35-45%) and not changing drastically in different plumes (Table S1). Based on these examples, we conclude that the reason for the differing MEE values under different air mass types is primarily differences in the corresponding aerosol size distributions.~~

5 Next we examine the similarity of MEE values observed in the Colorado Front Range to previous measurements. MEE is the sum of the mass absorption and scattering efficiencies (MAE and MSE respectively), which both depend on particle size, refractive index, and wavelength of light (Seinfeld et al. 2006). Keeping in mind that in the presence of absorbing species, MEE is higher than mass scattering efficiency (MSE), in the absence of estimates of MEE in other regions, we present estimates of MSE from previous studies for comparison with the current MEE estimates in the Front
10 Range. PM_{2.5} scattering efficiencies at 550 nm in several ground based studies in urban commercial/ residential sites have typically been measured to be in the range of 2-3 m² g⁻¹ in (Chow et al. 2002, Hand et al. 2007). In such studies, the main aerosol sources contributing to the observed PM₁ MSE were the automotive emissions and combustion processes. Although the contribution of elemental or black carbon to PM₁ mass during FRAPPE is unknown, similar to these previous studies, OA contributed the most to the NR-PM₁ mass in the Front Range and in comparison, the observed average MEE values
15 value (2.24 ± 0.71 m² g⁻¹) ~~isare~~ consistent with the previous estimates of MSE.

3.4 Impacts of biomass burning (BB) emissions on optical extinction

During August 11 and 12, several wildfires were observed at Rocky Mountain National Park, near Tonahutu Creek Trail, 60 miles NW of Denver and Grand Mesa, Uncompahgre and Gunnison National Forest. BB gas-phase markers, namely hydrogen cyanide (HCN) and acetonitrile (CH₃CN) from TOGA and PTR-MS airborne data, respectively, were elevated in
20 the boundary layer throughout the flights on Aug. 11-12 compared to non-biomass burning days (July 26, 29, 31 and August 2-3, 7-8, 15-16, 18). For example, during the BB days, HCN (CH₃CN) mean mixing ratio in the boundary layer was 516 ± 58 pptv (201 ± 44 pptv) whereas the boundary layer mean mixing ratio on non-BB days was 327 ± 59 pptv (148 ± 38 pptv). Since elevated levels of HCN and CH₃CN were not observed in individual plumes but rather throughout the boundary layer on Aug. 11-12, a regional influence of biomass burning emissions was suspected to be present in the Front Range during this
25 time. In addition, a 25 ppbv increase in CO background values were observed on Aug. 11-12 (Figure S3) compared to non-BB days. Ground-based measurements of PM_{2.5} from Denver-La Casa (39.78 N, -105.01W), Denver-CAMP (39.75 N, -104.99 W), and Denver-I25 (39.73 N, -105.02 W) sites were analyzed to assess the regional impact of wildfire emissions in the Front Range ~~to in terms of the contribution of~~ PM_{2.5} during ~~the BB and non-BB the days of BB and non-BB~~. The time series of PM_{2.5} mass concentrations at the sites described above, during days preceding and following the wildfires shows
30 increases in mass concentration for PM_{2.5} during the days of BB (Figure ~~S6~~S4). The mean PM_{2.5} mass concentrations during the times of 9 am to 7 pm local time at Denver, La Casa, Denver-CAMP, and Denver-I25 during ~~non-BB~~non-biomass burning days were 5.61 ± 2.02, 6.01 ± 3.52, and 7.28 ± 2.91 μg m⁻³, while mean mass concentrations increased to 9.47 ± 2.05, 11.51 ± 3.04, and 14.08 ± 4.68 μg m⁻³, respectively, during the ~~BB~~biomass burning days. As seen in Figure ~~7~~6, the average

daytime PM_{2.5} mass concentration on BB days increased by 75-98% compared to the non-BB days confirming the regional influence of wildfires on the Front Range aerosol loadings.

In addition to scattering of light by smoke particles, BB emissions of black carbon (BC) and brown carbon (BrC) can lead to significant absorption of the solar radiation in the visible and UV region; at 632 nm absorption by BrC is minimal (Lack et al. 2012, May et al. 2014). ~~During Aug. 11-12, background values of airborne β_{ext} were higher by 10-15 Mm^{-1} , suggesting the additional contribution to β_{ext} from the wildfires. MEE values and $\Delta\beta_{\text{ext}}/\Delta\text{CO}$ enhancement ratios~~ were analyzed for days with and without the BB influence, using weighted linear ODR fit analysis, as explained previously. As seen in Figure 87, ~~average MEE and $\Delta\beta_{\text{ext}}/\Delta\text{CO}$ on Aug. 11-12 were was ~ 637030% and a factor of 5 two greater, respectively,~~ compared to days without the influence of BB ($3.65 \pm 1.16 \text{ m}^2 \text{ g}^{-1}$ vs. $2.2416 \pm 0.7168 \text{ m}^2 \text{ g}^{-1}$). ~~Additionally, during Aug. 11-12, background value of airborne β_{ext} was higher at $4.00 \pm 0.71 \text{ Mm}^{-1}$ compared to $0.25 \pm 0.117 \text{ Mm}^{-1}$ on days without the BB influence, suggesting the additional contribution to β_{ext} from the wildfires.~~ Although the AMS does not detect refractory materials such as BC due to the relatively low temperature of its vaporizer (600 °C), it is likely that on Aug. 11-12, BC emissions from the fires had resulted in elevated extinction values on a regional scale, resulting in higher MEE ~~and $\Delta\beta_{\text{ext}}/\Delta\text{CO}$~~ . The observed increase in MEE ~~and $\Delta\beta_{\text{ext}}/\Delta\text{CO}$~~ on Aug. 11-12 suggest that regional BB emissions have at least a comparable impact on aerosol optical extinction and visibility in the Front Range relative to the local sources.

4 Conclusions

Airborne aerosol optical extinction (632 nm) and submicron non-refractory aerosol composition were measured during the summer in the Colorado Front Range to understand sources and processes that impact summertime visibility in the area. In assessing the role of atmospheric processing on β_{ext} , $\Delta\beta_{\text{ext}}/\Delta\text{CO}$ enhancement ratio increased under aged urban air masses by ~54%. The increase in $\Delta\beta_{\text{ext}}/\Delta\text{CO}$ in the aged air masses was accompanied by a factor of ~5 increase in $\Delta\text{OA}/\Delta\text{CO}$, indicating that secondary formation of organic aerosols had significant impacts on the evolution of urban β_{ext} in the Front Range. Correlation between β_{ext} vs organic, nitrate, and sulfate aerosol mass under urban, O&G, agriculture, and urban + O&G mixed source influence were analyzed by linear regression fits. β_{ext} best correlated with organic aerosols under the O&G emissions and best correlated with nitrate aerosols under the O&G and agriculture influences. Correlation with sulfate was poor under all air mass types. Estimated average non-refractory mass extinction efficiency values for different air mass types ranged from $1.51 \pm 0.49 \text{ m}^2 \text{ g}^{-1}$ to $2.27 \pm 0.83 \text{ m}^2 \text{ g}^{-1}$, with the minimum and maximum average values observed in urban and agriculture air masses, respectively. Finally, aerosol components emitted from wildfires during the days of August 11 and 12 increased β_{ext} background values by ~4 Mm^{-1} and resulted in higher average MEE values by about 63% compared to non-biomass burning days, indicating that summertime visibility in the Front Range may equally be impacted by regional wildfires in addition to local sources.

Acknowledgments

The authors thank Daniel Adams (UCR's CNAS Machine Shop) and technicians at the NCARs Research Aviation Facility for integration of the instruments on the aircraft rack, a smooth aircraft integration process, and support throughout the project, Joshua Schwarz (NOAA-ESRL) for providing us the aircraft inlet system, Ron Cohen and Carly Ebben for providing the TD-LIF data, the Colorado Department of Public Health and Environment for funding and ground-based PM data, as well as the *USDA National Institute of Food and Agriculture, Hatch project Accession No. 233133* for additional funding support. Data used in this analysis may be obtained at <http://www-air.larc.nasa.gov/cgi-bin/ArcView/discover-aq.co-2014?C130=1>.

10 References

- Apel, E. C., et al. (2015). "Upper tropospheric ozone production from lightning NO_x-impacted convection: Smoke ingestion case study from the DC3 campaign." Journal of Geophysical Research-Atmospheres **120**(6): 2505-2523.
- Bahreini, R., et al. (2009). "Organic aerosol formation in urban and industrial plumes near Houston and Dallas, Texas." Journal of Geophysical Research-Atmospheres **114**.
- Bohren, C. F. and D. R. Huffman (1998). Absorption and Scattering of Light by Small Particles. New York, Wiley.
- Borbon, A., et al. (2013). "Emission ratios of anthropogenic volatile organic compounds in northern mid-latitude megacities: Observations versus emission inventories in Los Angeles and Paris." Journal of Geophysical Research-Atmospheres **118**(4): 2041-2057.
- Chow, J. C., et al. (2002). "Comparability between PM_{2.5} and particle light scattering measurements." Environmental Monitoring and Assessment **79**(1): 29-45.
- Crook, N. A., et al. (1990). "THE DENVER CYCLONE .1. GENERATION IN LOW FROUDE-NUMBER FLOW." Journal of the Atmospheric Sciences **47**(23): 2725-2742.
- Day, D. A., et al. (2002). "A thermal dissociation laser-induced fluorescence instrument for in situ detection of NO₂, peroxy nitrates, alkyl nitrates, and HNO₃." Journal of Geophysical Research-Atmospheres **107**(D5-6).
- de Gouw, J. and C. Warneke (2007). "Measurements of volatile organic compounds in the earths atmosphere using proton-transfer-reaction mass spectrometry." Mass Spectrometry Reviews **26**(2): 223-257.
- DeCarlo, P. F., et al. (2010). "Investigation of the sources and processing of organic aerosol over the Central Mexican Plateau from aircraft measurements during MILAGRO." Atmospheric Chemistry and Physics **10**(12): 5257-5280.
- Ellis, R. A., et al. (2010). "Characterizing a Quantum Cascade Tunable Infrared Laser Differential Absorption Spectrometer (QC-TILDAS) for measurements of atmospheric ammonia." Atmospheric Measurement Techniques **3**(2): 397-406.
- Ely, D. W., et al. (1993). The establishment of the Denver visibility standard. Air And Waste Management Association Annual Meeting, Air And Waste Management Association. **1**.

- Gerbig, C., et al. (1999). "An improved fast-response vacuum-UV resonance fluorescence CO instrument." Journal of Geophysical Research-Atmospheres **104**(D1): 1699-1704.
- 5 Gilman, J. B., et al. (2013). "Source Signature of Volatile Organic Compounds from Oil and Natural Gas Operations in Northeastern Colorado." Environmental Science & Technology **47** 1297–1305.
- Groblicki, P. J., et al. (1981). "VISIBILITY-REDUCING SPECIES IN THE DENVER BROWN CLOUD .1. RELATIONSHIPS BETWEEN EXTINCTION AND CHEMICAL-COMPOSITION." Atmospheric Environment **15**(12): 2473-2484.
- 10 Hand, J. L. and W. C. Malm (2007). "Review of aerosol mass scattering efficiencies from ground-based measurements since 1990." Journal of Geophysical Research-Atmospheres **112**(D18).
- Hobbs, P. V. (2000). Introduction to Atmospheric Chemistry: A Companion Text to Basic Physical Chemistry for the
15 Atmospheric Sciences. Cambridge, Cambridge UP.
- Huey, L. G. (2007). "Measurement of trace atmospheric species by chemical ionization mass spectrometry: Speciation of reactive nitrogen and future directions." Mass Spectrometry Reviews **26**(2): 166-184.
- 20 Huey, L. G., et al. (1998). "Fast time response measurements of HNO₃ in air with a chemical ionization mass spectrometer." Journal of Geophysical Research-Atmospheres **103**(D3): 3355-3360.
- Jayne, J. T., et al. (2000). "Development of an aerosol mass spectrometer for size and composition analysis of submicron particles." Aerosol Science and Technology **33**(1-2): 49-70.
- 25 Karl, T., et al. (2009). "Emissions of volatile organic compounds inferred from airborne flux measurements over a mega city." Atmos. Chem. Phys. **9**(1): 271-285.
- Kleinman, L. I., et al. (2007). "Aircraft observations of aerosol composition and ageing in New England and Mid-Atlantic States during the summer 2002 New England Air Quality Study field campaign." Journal of Geophysical Research-Atmospheres **112**(D9).
- 30 Lack, D. A., et al. (2012). "Brown carbon and internal mixing in biomass burning particles." Proc Natl Acad Sci U S A **109**(37): 14802-14807.
- 35 Langridge, J. M., et al. (2012). "Evolution of aerosol properties impacting visibility and direct climate forcing in an ammonia-rich urban environment." Journal of Geophysical Research: Atmospheres **117**(D21): n/a-n/a.
- Langridge, J. M., et al. (2011). "Aircraft Instrument for Comprehensive Characterization of Aerosol Optical Properties, Part I: Wavelength-Dependent Optical Extinction and Its Relative Humidity Dependence Measured Using Cavity Ringdown Spectroscopy." Aerosol Science and Technology **45**(11): 1305-1318.
- 40 Levin, E. J. T., et al. (2009). "Aerosol physical, chemical and optical properties during the Rocky Mountain Airborne Nitrogen and Sulfur study." Atmospheric Environment **43**(11): 1932-1939.
- 45 Malm, W. C. (1989). "Atmospheric Haze-Its Sources and Effects on Visibility in Rural Areas of the Continental United States." Environmental Monitoring and Assessment **12**(3): 203-225.
- 50 Massoli, P., et al. (2009). "Aerosol optical and hygroscopic properties during TexAQs-GoMACCS 2006 and their impact on aerosol direct radiative forcing." Journal of Geophysical Research-Atmospheres **114**.

- Massoli, P., et al. (2010). "Aerosol Light Extinction Measurements by Cavity Attenuated Phase Shift (CAPS) Spectroscopy: Laboratory Validation and Field Deployment of a Compact Aerosol Particle Extinction Monitor." Aerosol Science and Technology **44**(6): 428-435.
- 5 May, A. A., et al. (2014). "Aerosol emissions from prescribed fires in the United States: A synthesis of laboratory and aircraft measurements." Journal of Geophysical Research-Atmospheres **119**(20): 11826-11849.
- Middlebrook, A. M., et al. (2012). "Evaluation of Composition-Dependent Collection Efficiencies for the Aerodyne Aerosol Mass Spectrometer using Field Data." Aerosol Science and Technology **46**(3): 258-271.
- 10 Neff, W. D. (1997). "The Denver Brown Cloud studies from the perspective of model assessment needs and the role of meteorology." Journal of the Air & Waste Management Association **47**(3): 269-285.
- 15 Park, R. J., et al. (2003). "Sources of carbonaceous aerosols over the United States and implications for natural visibility." Journal of Geophysical Research-Atmospheres **108**(D12).
- Pétron, G., et al. (2014). "A New Look at Methane and Nonmethane Hydrocarbon Emissions from Oil and Natural Gas Operations in the Colorado Denver-Julesburg Basin." Journal of Geophysical Research-Atmospheres **119**(11): 6836-6852.
- 20 Petzold, A., et al. (2013). "Intercomparison of a Cavity Attenuated Phase Shift-based extinction monitor (CAPS PMex) with an integrating nephelometer and a filter-based absorption monitor." Atmospheric Measurement Techniques **6**(5): 1141-1151.
- Ramanathan, V., et al. (2001). "Atmosphere - Aerosols, climate, and the hydrological cycle." Science **294**(5549): 2119-2124.
- 25 Reddy, P. J., et al. (1995). "DEVELOPMENT OF A STATISTICAL-MODEL FOR FORECASTING EPISODES OF VISIBILITY DEGRADATION IN THE DENVER METROPOLITAN-AREA." Journal of Applied Meteorology **34**(3): 616-625.
- 30 Richter, D., et al. (2015). "Compact highly sensitive multi-species airborne mid-IR spectrometer." Applied Physics B-Lasers and Optics **119**(1): 119-131.
- Ridley, B. A. and F. E. Grahek (1990). "A SMALL, LOW FLOW, HIGH-SENSITIVITY REACTION VESSEL FOR NO CHEMILUMINESCENCE DETECTORS." Journal of Atmospheric and Oceanic Technology **7**(2): 307-311.
- 35 Rosenberg, P. D., et al. (2012). "Particle sizing calibration with refractive index correction for light scattering optical particle counters and impacts upon PCASP and CDP data collected during the Fennec campaign." Atmospheric Measurement Techniques **5**(5): 1147-1163.
- 40 Scamehorn, H. L. (2002). High Altitude Energy: A History of Fossil Fuels in Colorado. Boulder, CO. Colorado, University Press of Colorado.
- Schneider, W., et al. (1987). "ABSORPTION CROSS-SECTIONS OF NO₂ IN THE UV AND VISIBLE REGION (200 - 700 NM) AT 298-K." Journal of Photochemistry and Photobiology a-Chemistry **40**(2-3): 195-217.
- 45 Seinfeld, J. H. and S. N. Pandis (2006). Atmospheric chemistry and physics: from air pollution to climate change. Hoboken, New Jersey, John Wiley and Sons, Inc.

Slusher, D. L., et al. (2004). "A thermal dissociation–chemical ionization mass spectrometry (TD-CIMS) technique for the simultaneous measurement of peroxyacyl nitrates and dinitrogen pentoxide." Journal of Geophysical Research: Atmospheres **109**.

5 Thornton, J. A., et al. (2000). "Atmospheric NO₂: In situ laser-induced fluorescence detection at parts per trillion mixing ratios." Analytical Chemistry **72**(3): 528-539.

Vu, K. T., et al. (2016). "Impacts of the Denver Cyclone on Regional Air Quality and Aerosol Formation in the Colorado Front Range during FRAPPÉ 2014 " Atmos. Chem. Phys. Discuss.

10

Warneke, C., et al. (2007) Determination of urban volatile organic compound emission ratios and comparison with an emissions database. J. Geophys. Res.- Atmos. **112**, DOI: 10.1029/2006JD007930

Watson, J. G., et al. (1998). Northern Front Range Air Quality Study Final Report, Colorado State University.

15

Weber, R. J., et al. (2016). "High aerosol acidity despite declining atmospheric sulfate concentrations over the past 15 years." Nature Geoscience **9**(4): 282-+.

20 Wolff, G. T., et al. (1981). "VISIBILITY-REDUCING SPECIES IN THE DENVER BROWN CLOUD .2. SOURCES AND TEMPORAL PATTERNS." Atmospheric Environment **15**(12): 2485-2502.

Ying, Q., et al. (2004). "Source apportionment of visibility impairment using a three-dimensional source-oriented air quality model." Environmental Science & Technology **38**(4): 1089-1101.

25 Zheng, W., et al. (2011). "Characterization of a thermal decomposition chemical ionization mass spectrometer for the measurement of peroxy acyl nitrates (PANs) in the atmosphere." Atmospheric Chemistry and Physics **11**(13): 6529-6547.

30 Figures

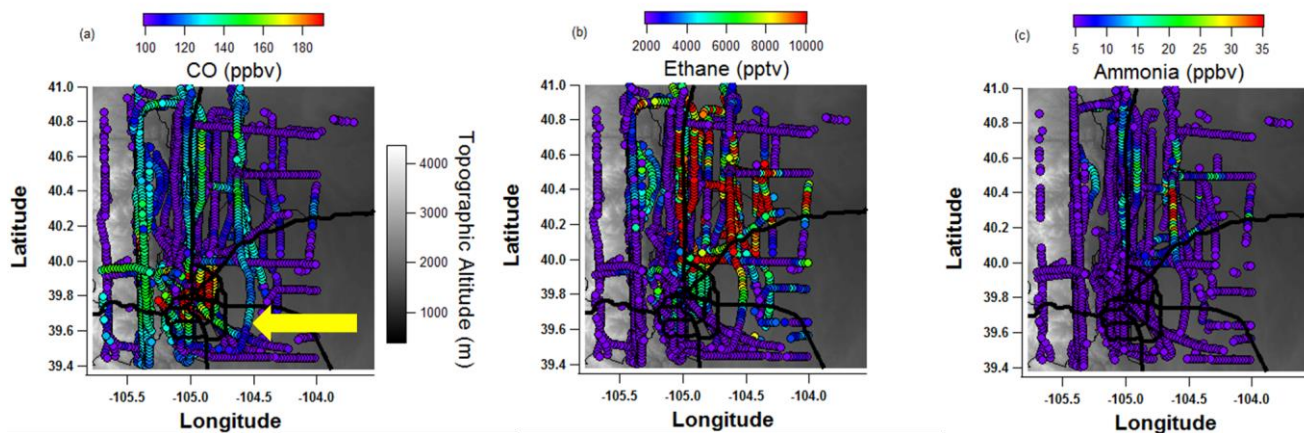
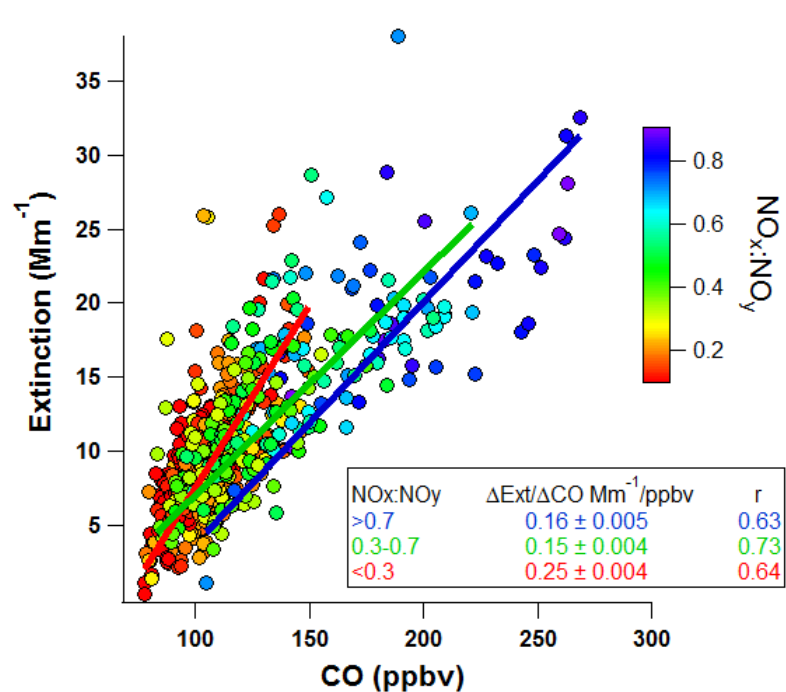


Figure 1. C-130 flight tracks in the Colorado Front Range, color coded with observed mixing ratios of (a) CO, (b) ethane, and (c) ammonia. The yellow arrow indicates the Denver metropolitan area. To the west of the Denver metropolitan area are the Rocky Mountain foothills depicted by the topographic color scheme.

5



10

Figure 2. Orthogonal distance linear regression fits to extinction (Mm^{-1}) vs. CO (ppbv) under fresh (blue fit line), intermediately aged (green fit line), and aged air masses (red fit line).

15

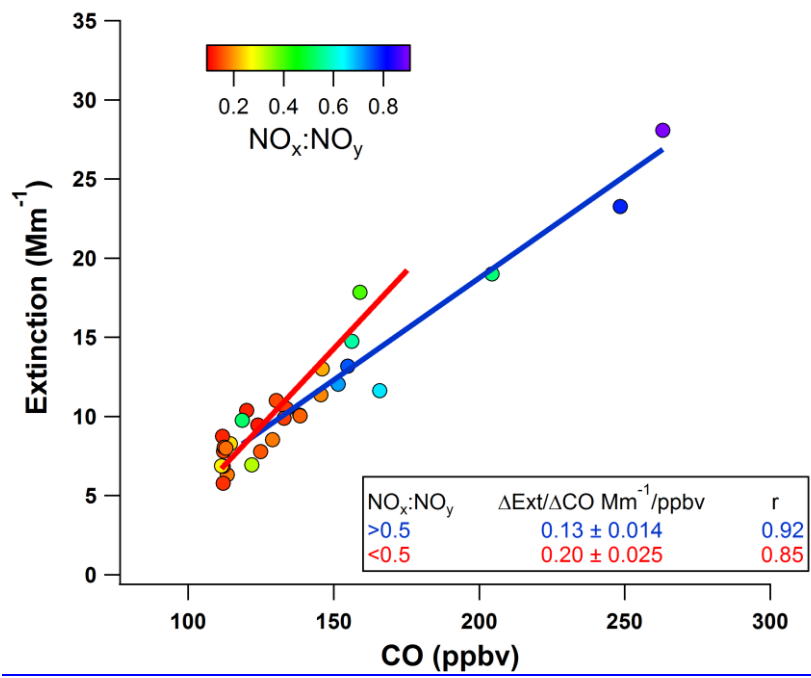
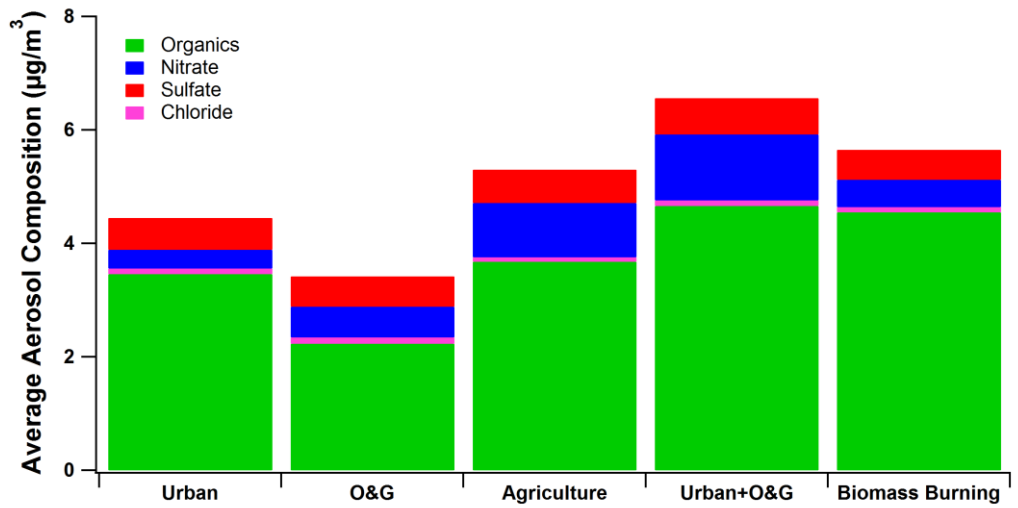
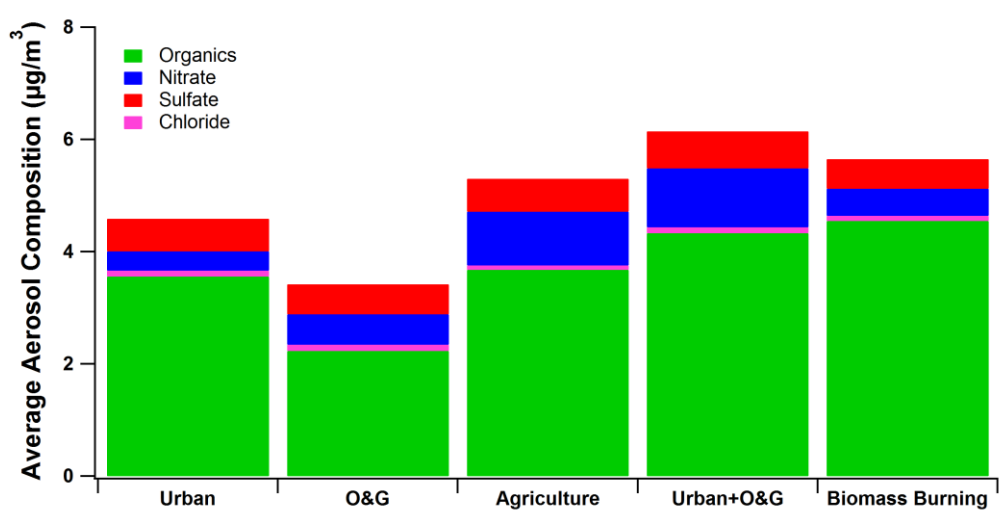


Figure 2. Orthogonal distance linear regression fits to extinction (Mm^{-1}) vs. CO (ppbv) under fresh (blue fit line) and aged air masses (red fit line).

5

10

15



[Figure 3. Average chemical composition \(\$\mu\text{g m}^{-3}\$ \) of non-refractory aerosols under different air mass source.](#)

5

10

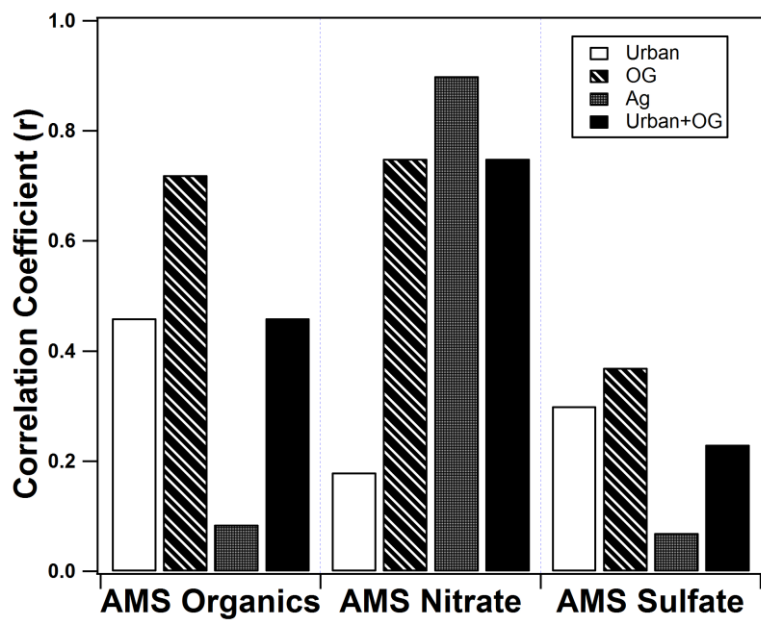
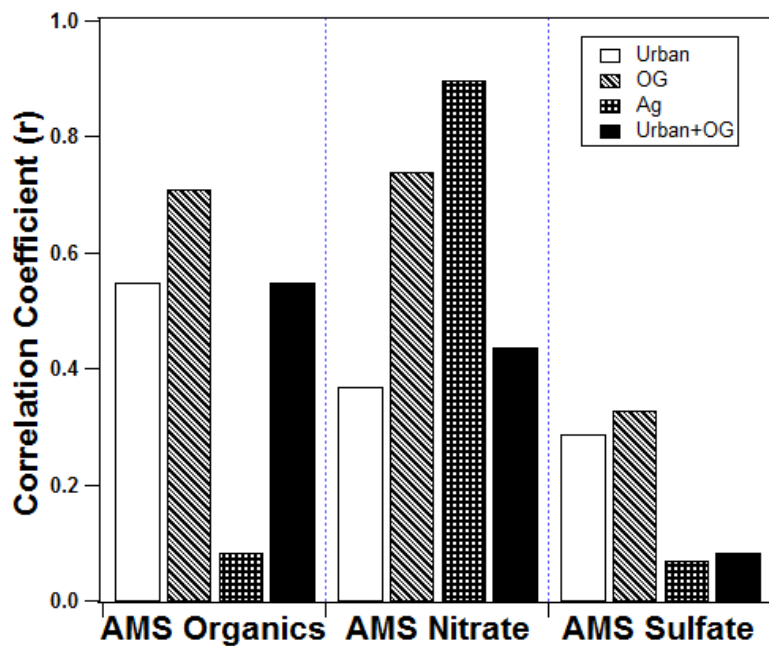
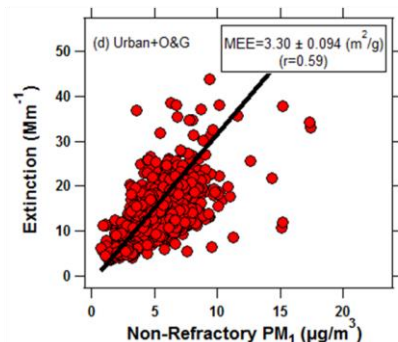
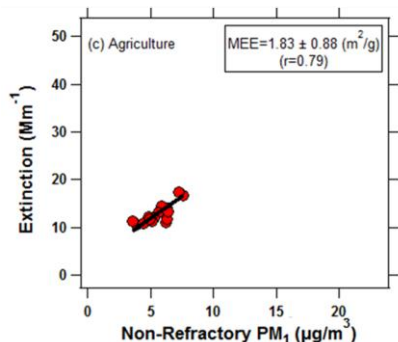
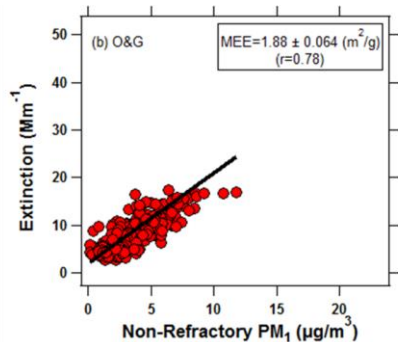
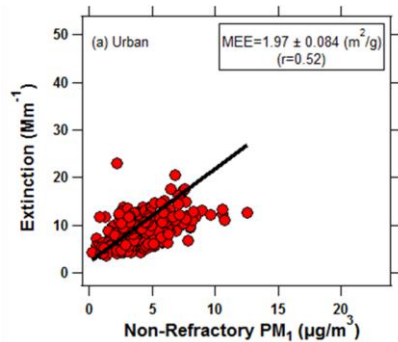


Figure 4. Correlations coefficients of β_{ext} vs. aerosol composition under urban, O&G, agriculture, urban + O&G emissions.



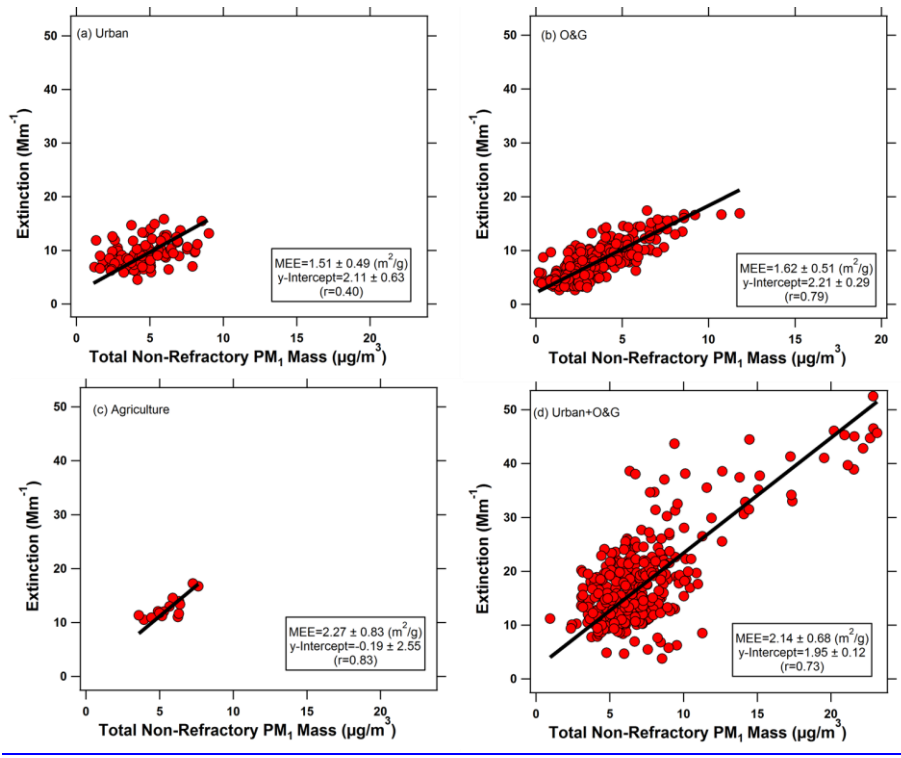


Figure 5. Mass extinction efficiencies (MEE) under (a) urban, (b) O&G, (c) agriculture, and (d) urban+O&G influence

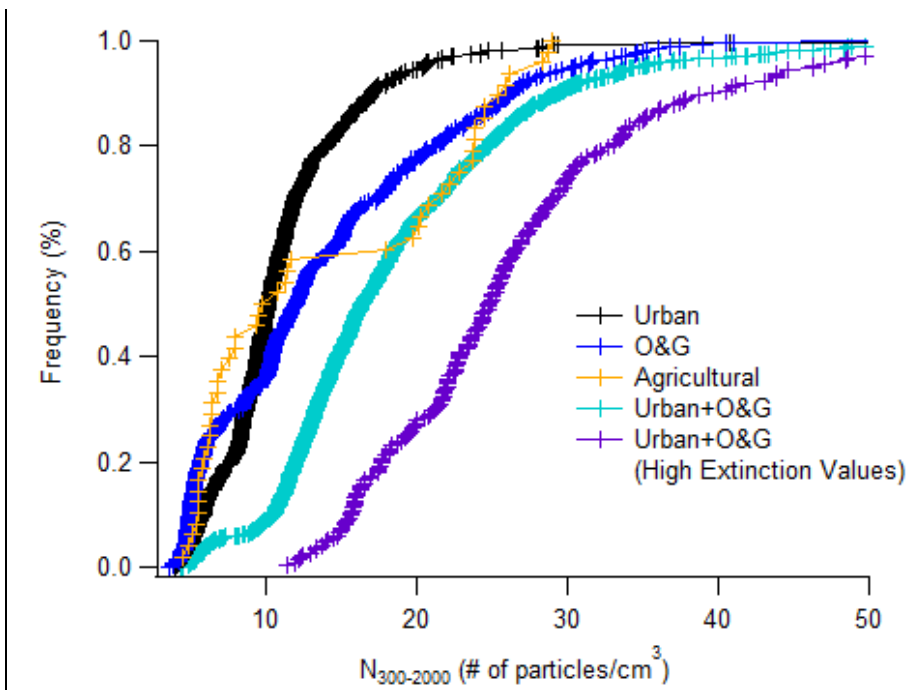


Figure 6. Cumulative particle number concentrations in the size range of 300-2000 nm in different air mass categories.

5

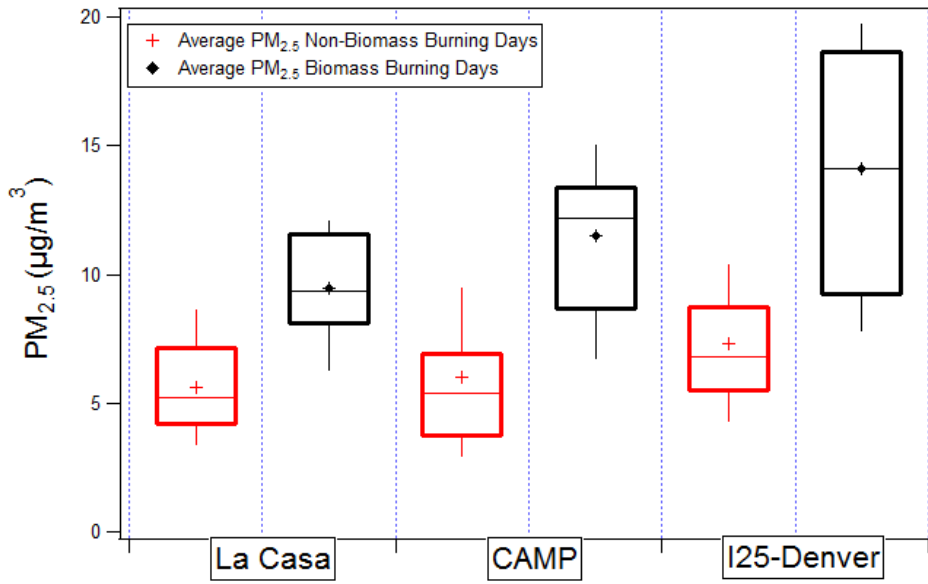
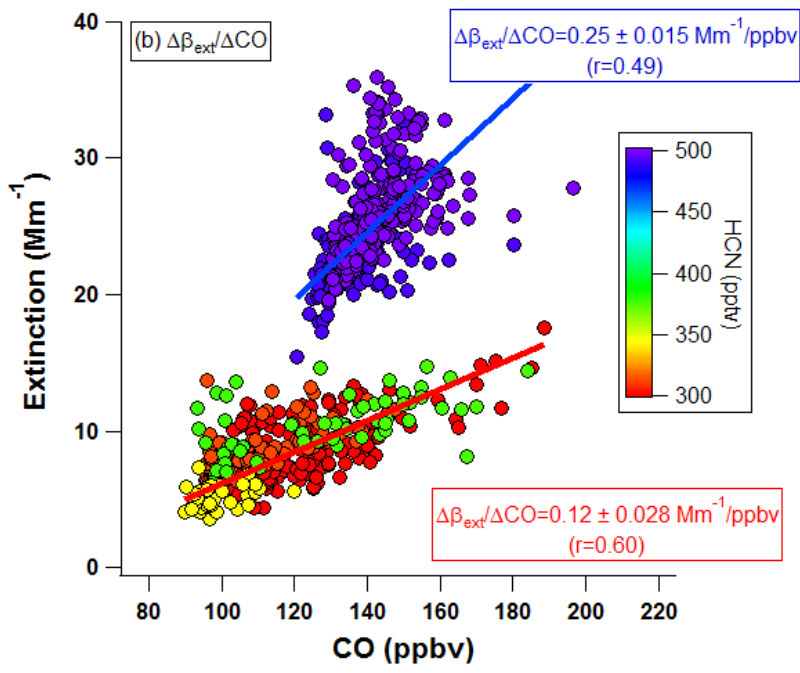
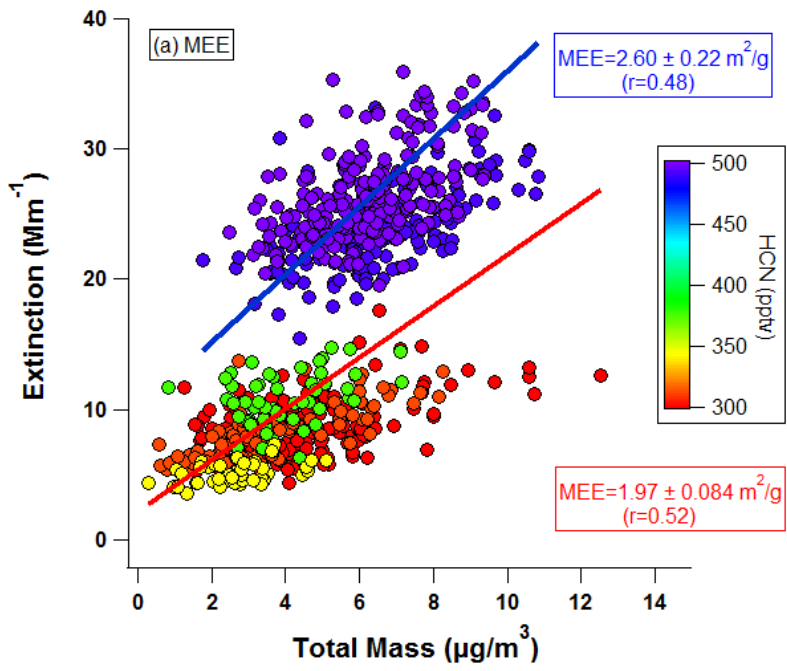


Figure 67. Daily (9 am - 7 pm local time) average $PM_{2.5}$ mass concentration for 3 monitoring sites for (a) non-biomass burning days of July 26, 29, 31 and August 02, 03, 07, 08, 15, 16, 18 and (b) biomass burning days of August 11 and 12. The whisker top, whisker bottom, box top and box bottom represents the 90th, 10th, 75th, and 25th percentiles.



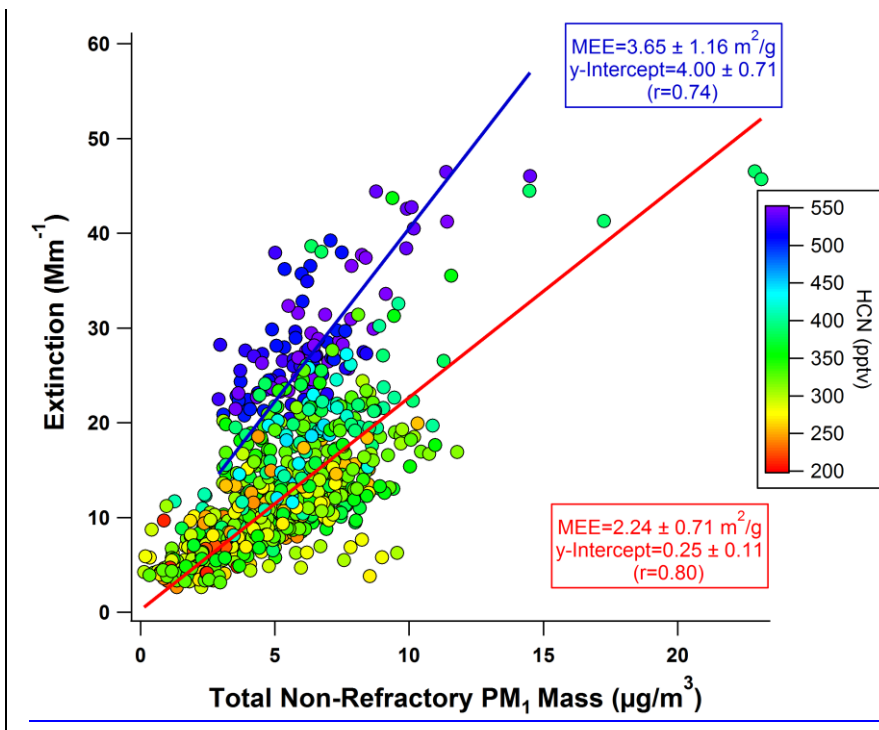


Figure 78. Orthogonal distance linear regression fits to ~~(a)~~ extinction (Mm⁻¹) vs. total NR-PM₁ mass (µg/m³) ~~and (b)~~ extinction (Mm⁻¹) vs. CO (ppbv). Data points are color coded with the average HCN mixing ratio for non-biomass burning and biomass burning days.

Supplementary materials for ACP manuscript: Aerosol Optical Extinction during the Front Range Air Pollution and Photochemistry Experiment (FRAPPÉ) 2014 Summertime Field Campaign, Colorado U.S.A.

5 Justin H. Dingle¹, Kennedy Vu¹, Roya Bahreini², Eric C. Apel³, Teresa L. Campos³, Frank Flocke³,
Alan Fried⁴, Scott Herndon⁵, Alan J. Hills³, Rebecca S. Hornbrook³, Greg Huey⁶, Lisa Kaser³, Denise
D. Montzka³, John B. Nowak⁵, Mike Reeves³, Dirk Richter⁴, Joseph R. Roscioli⁵, Stephen Shertz³,
Meghan Stell³, David Tanner⁶, Geoff Tyndall³, James Walega⁴, Petter Weibring⁴, Andrew
Weinheimer³

10

¹ Environmental Toxicology Graduate Program, University of California, Riverside, CA 92521

² Department of Environmental Sciences, University of California, Riverside, CA 92521

³ National Center for Atmospheric Research, Boulder, CO 80301

⁴ Institute for Arctic and Alpine Research, University of Colorado, Boulder, CO 80303

15 ⁵ Aerodyne Research, Inc., Billerica, MA 01821

⁶ Department of Earth and Atmospheric Sciences, Georgia Institute of Technology, Atlanta, GA 30033

Corresponding author: R. Bahreini (roya.bahreini@ucr.edu)

20 **Supplementary ~~Table and~~ Figures**

Air Mass Type	Mean Temperature (°C)	Mean Relative Humidity (%)
Urban	20.48 ± 5.57	36.85 ± 12.55
O&G	19.29 ± 5.98	39.65 ± 16.36
Agriculture	23.11 ± 3.71	38.98 ± 15.80
Urban+O&G	20.59 ± 3.53	45.91 ± 8.21

Table S1. Mean temperature and relative humidity under the urban, O&G, agriculture, and urban+O&G air mass types.

25

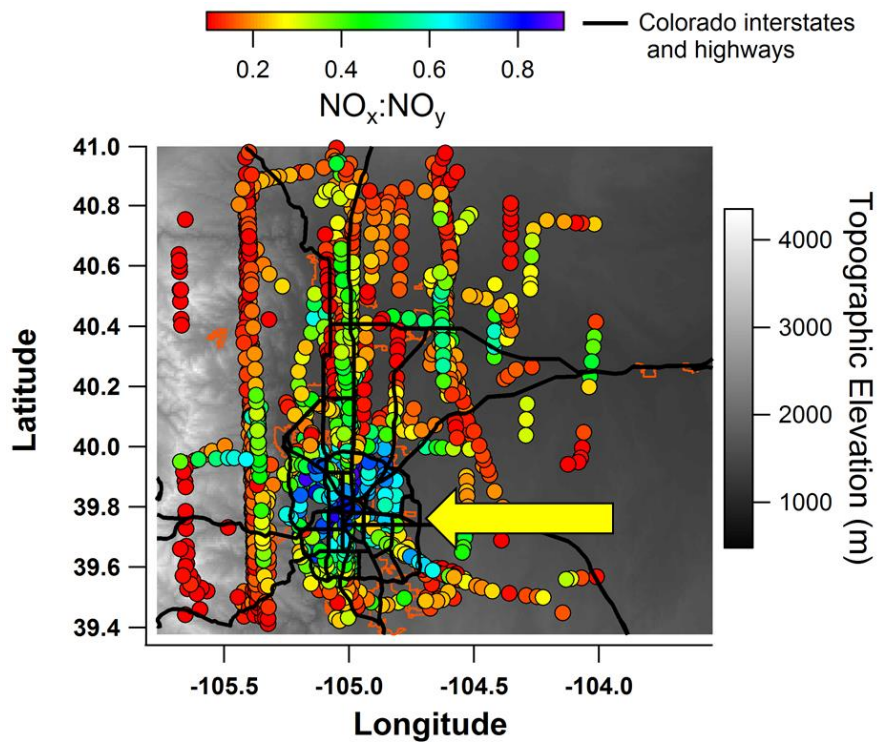
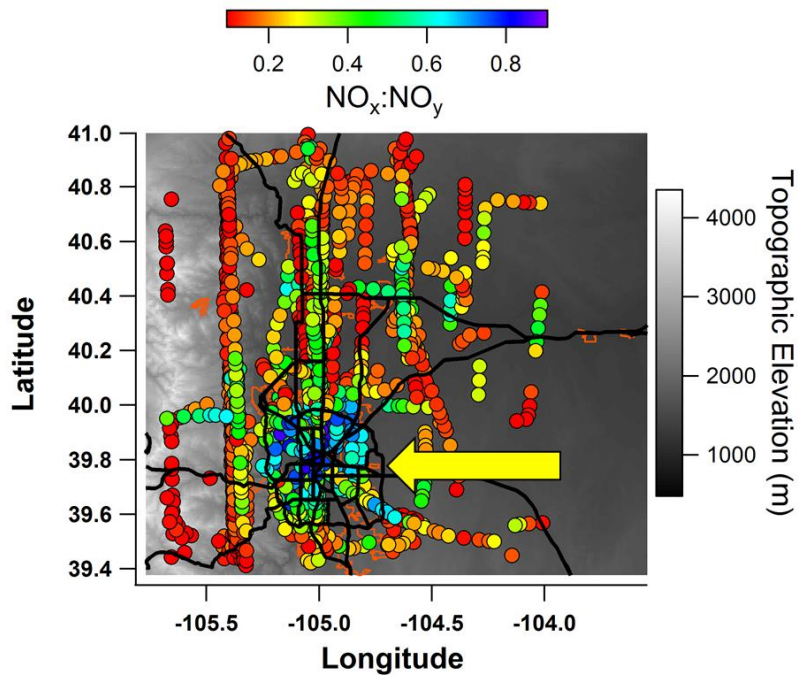
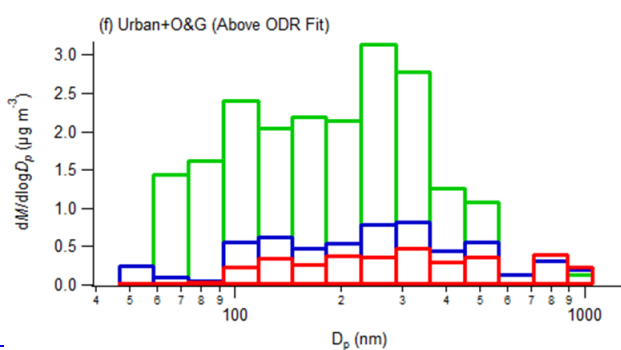
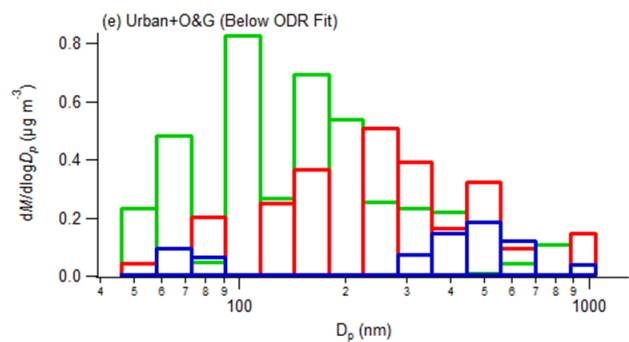
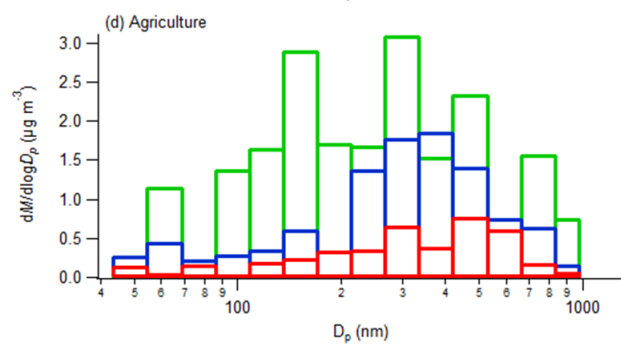
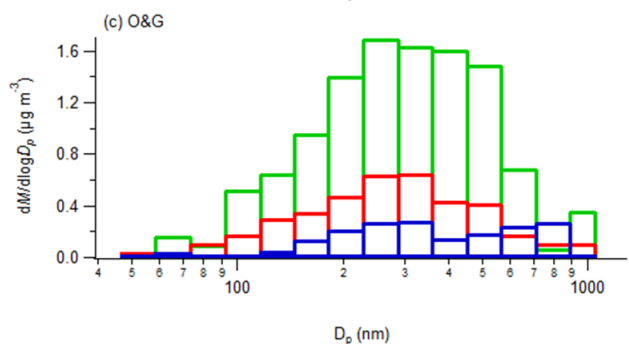
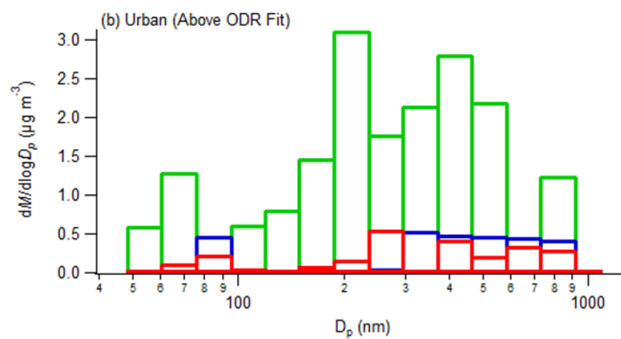
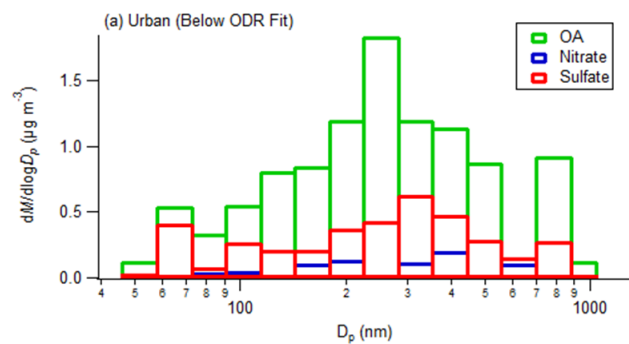


Figure S1. C-130 flight tracks in the Colorado Front Range, color coded by the observed $\text{NO}_x:\text{NO}_y$ ratio to examine the photochemical processing of the pollutants in the area during all flights excluding the days when the Denver Cyclone and biomass burning were experienced. The arrow indicates the Denver metropolitan area. To the west of the Denver metropolitan area are the Rocky Mountain foothills depicted by the topographic color scheme.



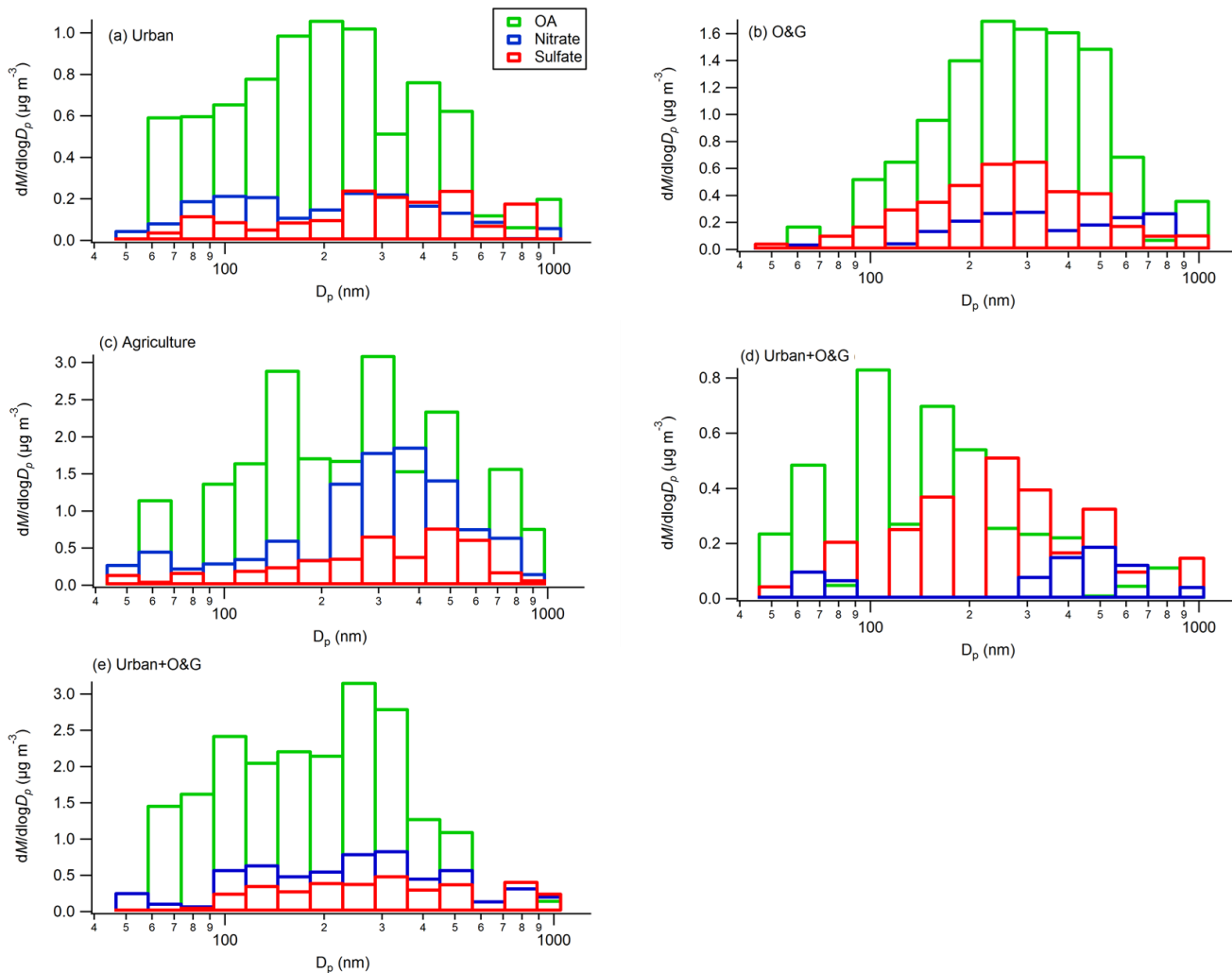


Figure S2. Aerosol mass distributions for OA (green), nitrate (blue), and sulfate aerosols under (a-b) urban, (c) O&G, (d) agriculture and (e-f) urban+O&G air masses.

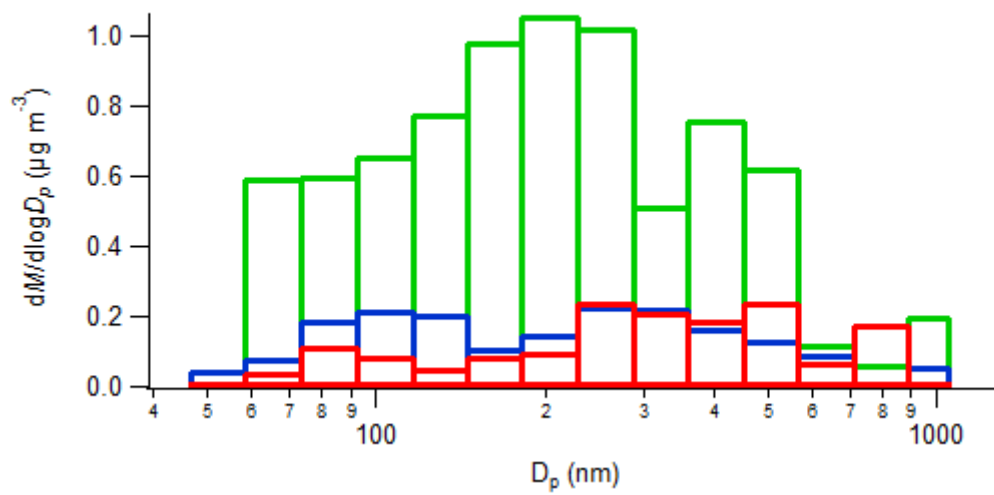
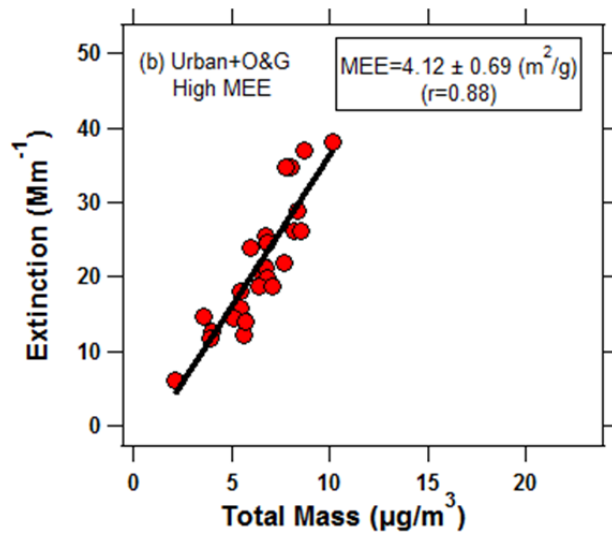
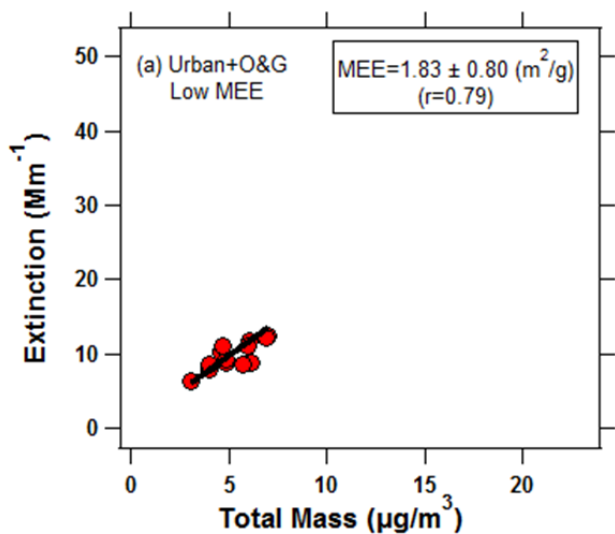
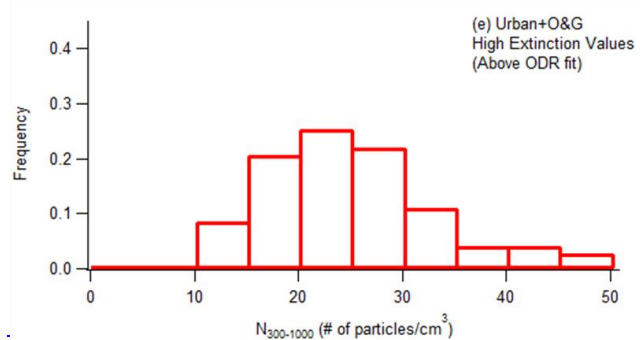
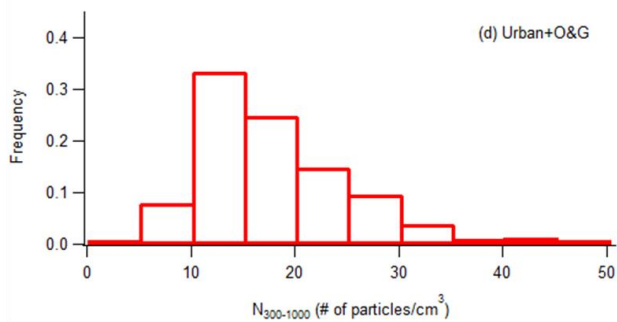
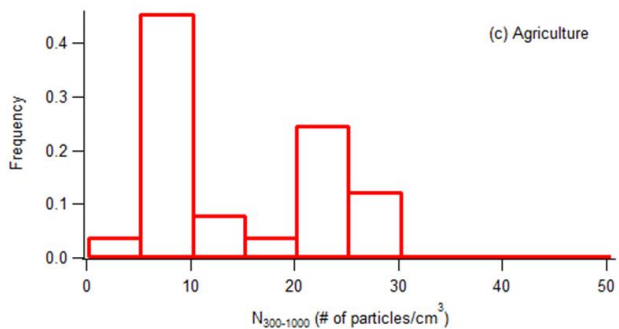
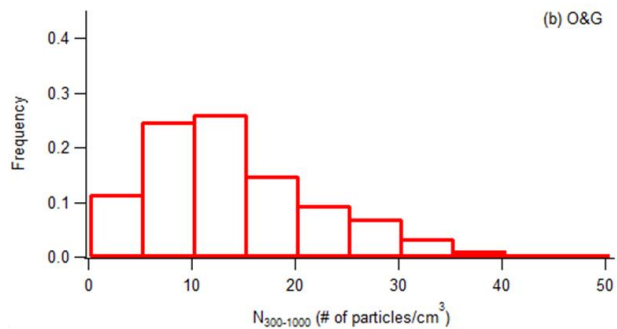
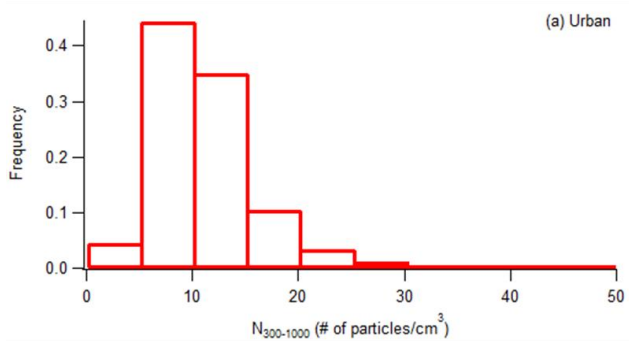


Figure S3. Mass distribution for an urban air mass for data points along the ODR fit line of Figure 4a from the Aug. 02 flight.



5

Figure S4. MEE for urban+O&G air masses with data points (a) below the ODR fit and (b) above the ODR fit in Figure 4d.



5 **Figure S5.** Frequency distributions of particle number concentrations in the size range of 300-1000 nm in different air masses from PCASP data in units of $\#/cm^3$.

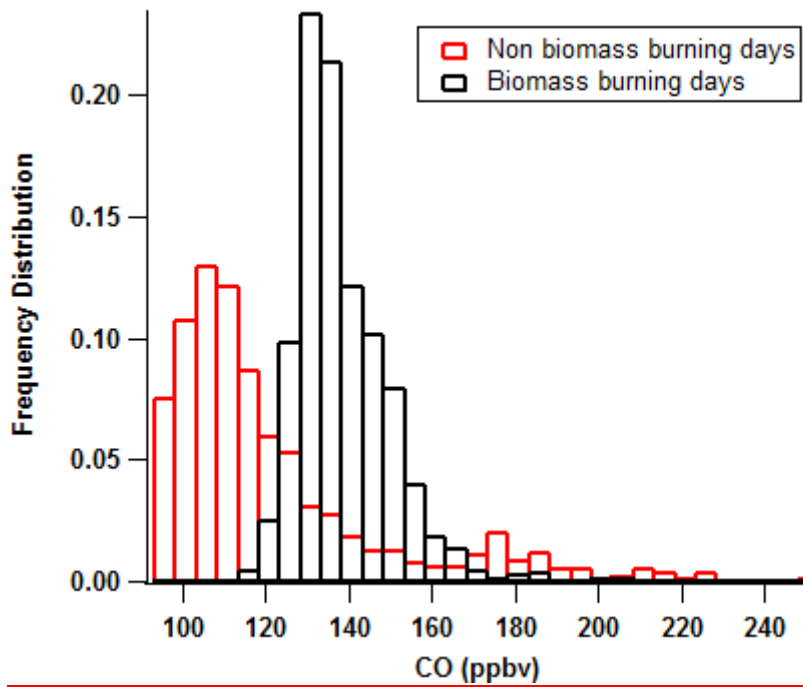


[Figure S4S3](#). Frequency histogram of CO in the Front Range during non-BB (red) and BB (black) days.

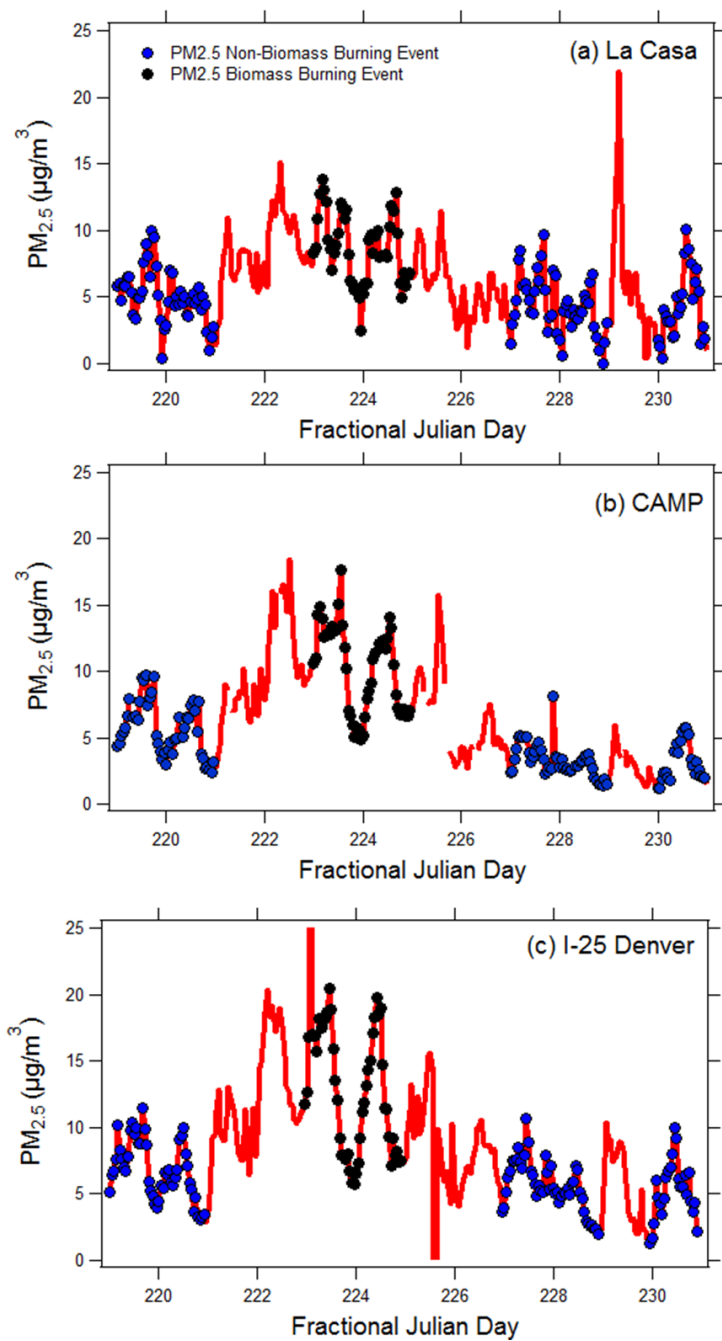


Figure S34. Time series for PM_{2.5} at La Casa (a), CAMP (b) and I-25 (c) ground sites located in the Front Range during July 26 - August 18. Markers highlight the periods corresponding to the C130 flights.